Geochemistry, Geophysics, Geosystems

RESEARCH ARTICLE
10.1029/2019GC008562

Progressive Changes in Magma Transport at the Active Serreta Ridge, Azores

R.H.W. Romer[1], C. Beier[1,2], K.M. Haase[1], A. Klügel[3], and C. Hamelin[4]

[1]GeoZentrum Nordbayern, Friedrich-Alexander-Universität Erlangen-Nürnberg, Erlangen, Germany, [2]Department of Geosciences and Geography, University of Helsinki, Helsinki, Finland, [3]Fachbereich Geowissenschaften, Universität Bremen, Bremen, Germany, [4]Department of Earth Science, University of Bergen, Bergen, Norway

Key Points:
- Azores volcanism occurs largely along WNW-ESE and NW-SE oriented structures from mantle melting along with transtensional tectonics
- Serreta Ridge mostly formed by lateral melt transport from a central volcano facilitated by tectonic pathways in the crust
- The youngest part of Serreta Ridge is the surface expression of a young plumbing system, heralding the formation of a new central volcano

Supporting Information:
- Supporting Information S1
- Table S1
- Table S2
- Table S3

Correspondence to:
R. H. W. Romer,
rene.romer@fau.de

Citation:
Romer, R. H. W., Beier, C., Haase, K. M., Klügel, A., & Hamelin, C. (2019). Progressive changes in magma transport at the active Serreta Ridge, Azores. *Geochemistry, Geophysics, Geosystems*, *20*, 5394–5414. https://doi.org/10.1029/2019GC008562

Received 9 JUL 2019
Accepted 22 SEP 2019
Published online 28 NOV 2019

Abstract Volcanism in the Eastern Azores Plateau occurs at large central volcanoes and along subaerial and submarine fissure zones, resulting from a mantle melting anomaly combined with transtensional stresses. Volcanic structures are aligned WNW-ESE and NW-SE, reflecting two tectonic stress fields that control the direction of lateral melt transport. Terceira Island is influenced by both stress fields, dividing the island into an eastern and western part. Several submarine volcanic ridges with variable orientations are located west of Santa Bárbara, the youngest central volcano on Terceira. Major, trace element and Sr-Nd-Pb-Hf isotope compositions from submarine lavas and glasses, in part associated with the 1998–2001 Serreta Ridge eruption, vary between different lava suites, suggesting a formation from different mantle sources. Submarine lavas are more primitive than those from Santa Bárbara volcano, indicating that they are not laterally connected with the shallow magma reservoir located in 2- to 5-km depth beneath the central volcano. Mineral thermobarometric data suggest that the older Serreta magmas were laterally transported at depths >5 km from Santa Bárbara predominantly in WNW direction. We propose that lithospheric extension controls magma transport from the central volcano to Serreta Ridge. The youngest Serreta lavas differ from Santa Bárbara and other submarine ridges in having less radiogenic Pb and higher Hf isotope ratios representing a new magma pulse ascending from the mantle. We conclude that lateral magma transport and the morphology of volcanic ridges are controlled by tectonic stresses in the lithosphere, whereas vertical melt transport is initiated by processes in the mantle.

Plain Language Summary The submarine eruption of lavas along elongated volcanic fissure zones close to volcanic oceanic islands provides the opportunity to chemically decipher the movement of magmas in the crust. Submarine samples from the active Serreta Ridge situated only some 10 km's west of the inhabited island of Terceira in the Azores show that the magmas were transported in the crust at depths of >5 km from the westernmost volcano Santa Bárbara to the site of eruption using pathways predefined by the Azores tectonic situation between the Eurasian and African plates. Lavas from the 1998–2001 eruption of Serreta Ridge, however, indicate that the youngest magmas ascended directly from the mantle through the crust independent of the existing crustal pathways. We interpret the changes in geochemical signals as a transgression from a fissure system being directly related to a central volcano to a new volcanic system acting as a precursor for the formation of a central volcanic edifice west of Santa Bárbara.

1. Introduction

The interaction between ascending magmas and extensional tectonic stresses commonly leads to formation of elongated volcanic fissure zones reflecting numerous repeated dike intrusion (Fiske & Jackson, 1972; Furumoto, 1978). In such environments, both magmatic and tectonic processes affect melt formation, ascent, temporary ponding, and finally eruption to varying extents (Garcia et al., 1996; Gudmundsson et al., 2014; Klügel, Hansteen, & Galipp, 2005). Tectonic stresses in particular define the pathways of ascending melts in the crust and are thus one major controlling factor on the morphology of the resulting volcanic structures, for example, volcanoes at oceanic spreading axes are commonly elongated reflecting the intrusion of kilometer long dikes and the formation of volcanic ridges (Smith & Cann, 1993). As a result of the interacting magmatic and tectonic processes the orientation of dikes, sills, volcanic cone alignments, and fault systems are commonly oriented perpendicular to the least compressive stress σ_3 (Walker, 1999) allowing to reconstruct how melts are transported in the crust.

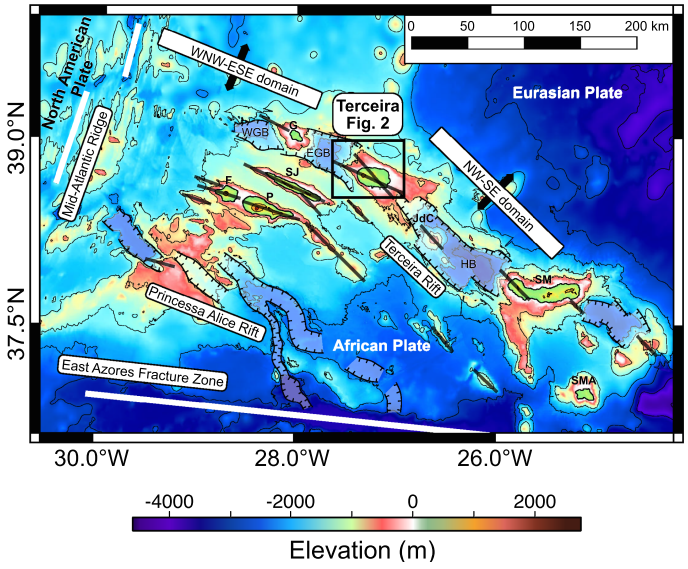

Figure 1. Map of the Eastern Azores Plateau with major tectonic boundaries (contours are 1,000-m elevation) using grids from R/V Meteor and R/V Poseidon cruises M79, Pos232, Pos286, M113 (Hübscher et al., 2016), and M128 (Beier et al., 2017) and bathymetric metadata and digital terrain model data from the EMODnet Bathymetry portal—http://www.emodnet-bathymetry.eu. The black solid lines indicate the orientation of volcanic structures on the islands and submarine ridges. They are separating the Eastern Azores Plateau into a western (WNW-ESE domain) and an eastern (NW-SE domain) part with distinct preferred orientations. Note that the distinct orientations are a spatial rather than a temporal effect because young <100 ka volcanism occurred along structures from both stress domains. The black box shows the extend of Figure 2a. Structural features (WGB: Western Graciosa Basin; EGB: Eastern Graciosa Basin; HB: Hirondelle Basin) and volcanic islands and seamounts (SM: São Miguel; SMA: Santa Maria; P: Pico; F: Faial; SJ: São Jorge; G: Graciosa; JdC: D. João de Castro seamount) are labelled with abbreviations.

Fissure zones, marked by linear alignments of eruptive centers, fissures and dike swarms are often associated with the large crustal magmatic system of a central volcano. Studies on Iceland (Gudmundsson, 2000), Hawaii (Tilling & Dvorak, 1993) and Fernandina (Geist et al., 2006) show that dike swarms of central volcanoes are often fed laterally from a shallow crustal magma reservoir. Lateral magma transport in the (shallow) crust along sills and dikes depends on the local and regional stress fields, as well as on the mechanical properties of crustal layers (Gudmundsson, 2006). The isotopic composition of lavas erupted from fissure zones and from the corresponding central volcano will be similar if they are fed from the same magma reservoir. Sigmarsson and Halldórsson (2015) used Sr and Nd isotope ratios to show that on the neighboring Icelandic Bardarbunga and Askja volcanic systems each central volcano and its associated dike swarm eruptions are isotopically similar and thus derived from the same source. Contrastingly, the Bardarbunga and Askja volcanic systems are isotopically distinct from each other, showing that both central volcanoes have independent plumbing systems and tap compositionally distinct sources. Studies on the Azores also show that focused melt transport can result in volcanic rift structures with distinct lava compositions on a spatial scale of less than few kilometers (Romer et al., 2018).

On Hawaii Big Island, the evolution of the Kilauea volcanic system displays a notable progressive change in the mantle source composition since CE 1960 based on trace element and Sr-Nd-Pb isotope ratios (Pietruszka et al., 2018). However, most eruptions from Kilauea above a shallow summit reservoir are associated with imminent volcanic activity along the fissure zones with lavas that have a similar isotopic composition. This suggests that melts that are laterally transported over several tens of kilometers from a shallow summit reservoir along fissure zones are able to preserve the isotopic signature of the magmatic system.

The submarine volcanic systems and islands from the Azores archipelago are strongly influenced by extension of the lithosphere above a mantle melting anomaly (Beier et al., 2008; Gente et al., 2003; Vogt & Jung, 2004), making them an ideal locality for studying volcano-tectonic interactions. The island of Terceira is ideally suited to investigate the relationship between a central volcano and associated submarine fissure zones, because the most recent volcanic activity in the Azores occurred between 1998 and 2001 at Serreta Ridge, located 10 km offshore the youngest central volcano (Santa Bárbara) of Terceira. This allows to temporarily correlate the formation of the Serreta Ridge and the Santa Bárbara volcano using geochemical and structural observations.

Here, we combine new major and trace element and Sr-Nd-Pb-Hf isotope data of glasses and lavas with clinopyroxene-melt thermobarometry and observations on the structural features from the submarine Serreta Ridge along with previously published data from Santa Bárbara central volcano. We show that the older parts of Serreta Ridge formed by lateral westward transport of melts over several tens of kilometers from Santa Bárbara. Similar lateral magma transport processes may also occur at other volcanic systems from the Azores, or other volcanic areas influenced by extensional/transtensional tectonic stresses. The most recent Serreta eruption, however, displays distinct trace element and isotope data indicating a vertical melt transport from the mantle. We develop a model in which the youngest eruption shows the presence of a young magmatic plumbing system underneath Serreta Ridge which may result in the formation of a new central volcanic system west of Santa Bárbara.

2. Geological Background

The Azores archipelago in the central Northern Atlantic is separated by the Mid-Atlantic Ridge (MAR) into an eastern and western part (Figure 1). The Azores Plateau formed from a melting anomaly in the mantle, either

due to a small thermal plume head (Cannat et al., 1999; Schilling, 1975; White et al., 1976) or from an anomalous volatile rich mantle (Asimow et al., 2004; Beier et al., 2012; Bonatti, 1990; Métrich et al., 2014; O'Neill & Sigloch, 2018; Schilling et al., 1980). The young volcanic islands of the eastern Azores (e.g., São Miguel, Terceira, and Graciosa; Figure 1) formed by volcanism along the Terceira Rift or its predecessors; only the older Santa Maria Island displays no obvious rift component. The Terceira Rift is an ultraslow oblique spreading axis, with a divergence rate of 2–4 mm/a (Vogt & Jung, 2004) forming part of the diffuse plate boundary between the Eurasian and African plates (Marques et al., 2013; Miranda et al., 2018; Sibrant et al., 2014). Islands and seamounts along the Terceira Rift are separated by deep non-volcanic basins (Beier et al., 2008; Figure 1). Islands along the Terceira Rift or along subparallel lineaments typically show an overall decrease of age of magmatic centers from the ESE to the WNW (e.g., Abdel-Monem et al., 1975; Calvert et al., 2006; Hildenbrand et al., 2008; Hildenbrand et al., 2012; Hildenbrand et al., 2014; Johnson et al., 1998; Moore, 1990; Nunes et al., 2014). Submarine fissure zones are located NW or WNW of most islands, extending from subaerial volcanic structures into the northwestern submarine basins, respectively (Beier et al., 2017; Casalbore et al., 2015; Casas et al., 2018; Hübscher et al., 2016; Romer et al., 2018; Weiß et al., 2015). Eruptions from volcanic fissure zones either occur subaerially on the islands or along the submarine island flanks forming several kilometer-long volcanic ridges. Volcanism at the central volcanoes and fissure zones in the eastern Azores is largely controlled by tectonic stresses, as is evident from the WNW-ESE and NW-SE elongated shaped islands and ridges (Hildenbrand et al., 2014; Lourenço et al., 1998). The dominant orientation of islands and ridges in the Azores varies systematically with respect to their distance from the MAR (Figure 1). The central Azores Islands (e.g., Faial, Pico, São Jorge and Graciosa) are located closer to the MAR and are predominantly oriented WNW-ESE. Conversely, islands, seamount and ridges (i.e., D. João de Castro seamount, Pico Ridge and the western part of São Miguel) that are located further from the MAR have a NW-SE orientation (Lourenço et al., 1998). The island of Terceira comprises two distinct major orientations (Madeira et al., 2015) because it is located on the boundary between the two stress domains (Lourenço et al., 1998; Marques et al., 2015).

Terceira is generally dominated by extension/transtension in WSW and ENE directions in the western part, and SW and NE directions in the eastern part (Lourenço et al., 1998; Marques et al., 2015; Figure 2). This results in WNW-ESE and NW-SE striking structural and volcanic features, respectively (Figure 2). The orientations of these structures continue offshore, in particular at two volcanic ridges that extend from the island in WNW (Serreta Ridge) and NW (NW Terceira Ridge) directions (Casalbore et al., 2015; Quartau et al., 2014). Terceira Island is formed by four central volcanoes and a young system of subaerial and submarine volcanic fissure zones. The central volcanoes are from east to west: Cinco Picos, Guilherme Moniz, Pico Alto and Santa Bárbara (Self, 1976). The oldest and easternmost Cinco Pico volcano (Figure 2a) was active >400 ka ago and is inactive (Calvert et al., 2006; Hildenbrand et al., 2014) whereas volcanic activity at Guilherme Moniz volcano lasted from >270 ka to 34 ka (Gertisser et al., 2010), and that of Pico Alto volcano probably lasted from ~140 ka (Gertisser et al., 2010) to <1 ka (Calvert et al., 2006).

Volcanic activity at the youngest and westernmost central volcano Santa Bárbara started 65 ka ago (Hildenbrand et al., 2014) and the youngest trachytic eruption occurred CE 1761 on the eastern flank of the volcano (Pimentel et al., 2016). Fissure zone volcanism began ~43 ka ago in the eastern part and <15 ka ago in the central and western part of Terceira, following a general SE-NW age progression of the subaerial fissure zone volcanism which is continued submarine at Serreta Ridge (Calvert et al., 2006; Zanon & Pimentel, 2015). The most recent volcanic eruption occurred between 1998 and 2001 along the southernmost segment of Serreta Ridge. The intermediate-depth Strombolian-style eruption was characterized by the intermittent emission of lava balloons and ash (Casas et al., 2018; Gaspar et al., 2003; Kueppers et al., 2012).

3. Sampling and Methods

3.1. Bathymetry and Sampling of the Volcanic Structures

Bathymetric data from Serreta Ridge (Serreta sub-ridge A [SR-A]; Figure 2) and N′ Serreta Ridges (Serreta sub-ridge B [SR-B] and Serreta sub-ridge C [SR-C]; Figure 2) were obtained during R/V *Meteor* cruises M113 (Hübscher et al., 2016) and M128 (Beier et al., 2017; Figure 2). The bathymetric data were obtained using the hull mounted EM122 and EM710 multi-beam systems with signal frequencies of 12 kHz and 70–100 kHz, respectively.

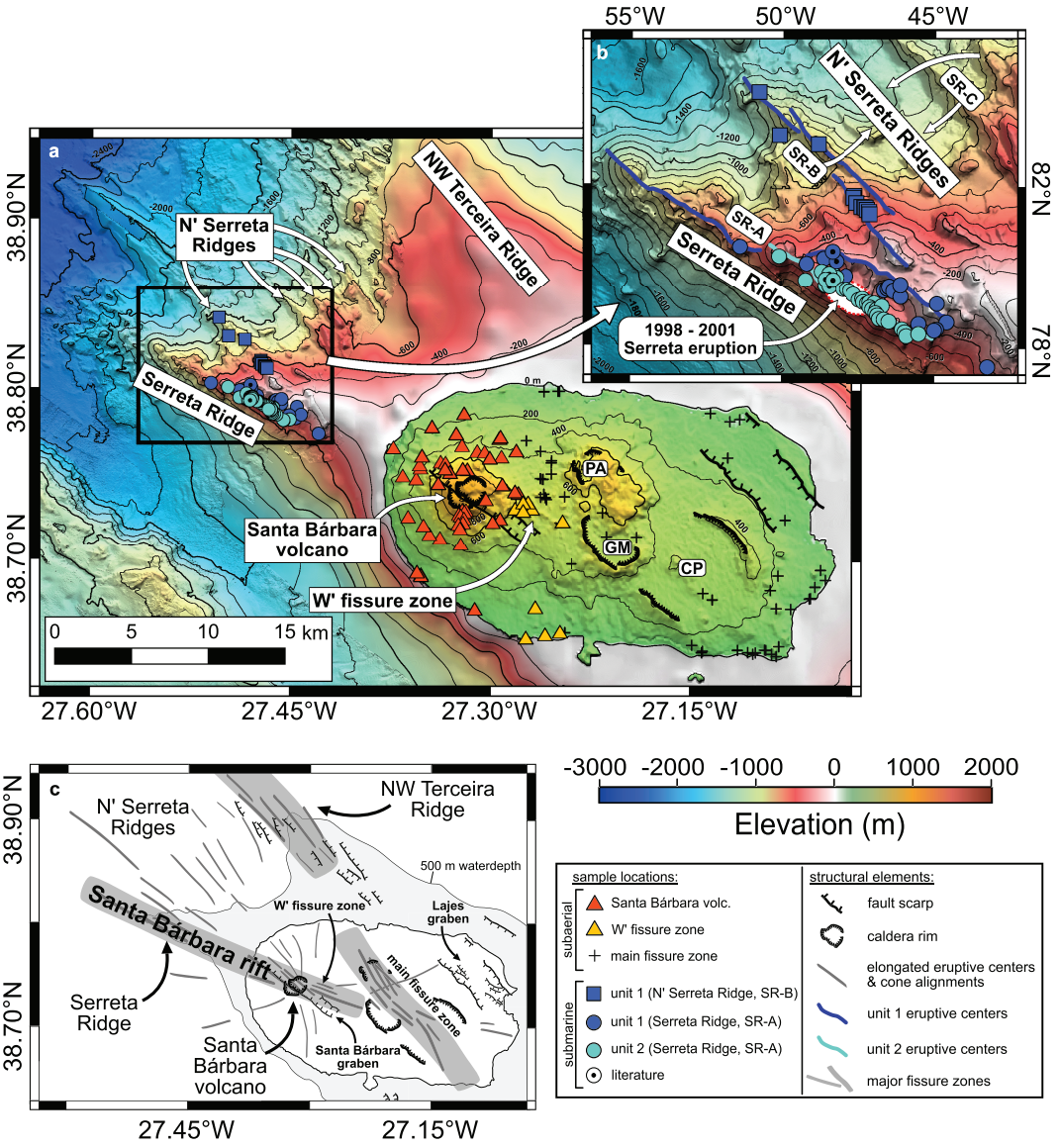

Figure 2. Map of (a) Terceira Island and its submarine volcanic fissure zones (contours are 200m). Subaerial central volcanos are labelled with abbreviations (CP: Cinco Picos; GM: Guilherme Moniz; PA: Pico Alto and; SB: Santa Bárbara). (b) Map of Serreta Ridge (Serreta sub-ridge A; SR-A) and the N′ Serreta Ridges (Serreta sub-ridge B [SR-B] and Serreta sub-ridge C [SR-C]; after Casas et al., 2018, and other, small unnamed ridges) with major elongated eruptive centers (contours are 100 m). White field highlights the area in which the 1998–2001 Serreta eruption occurred (Casas et al., 2018). Symbols in (a) and (b) mark sample localities of subaerial and submarine lavas. The classification of subaerial volcanic units is modified after Madureira et al. (2005). The submarine samples from Serreta Ridge (SR-A) and one N′ Serreta Ridge (SR-B) are subdivided based on structural features and their relative age into an older unit 1 (at SR-A and SR-B) and a younger unit 2 (only at SR-A). Location and orientation of the NW Terceira Ridge is from Quartau et al. (2014). (c) Simplified map of Terceira and surrounding seafloor with volcano-tectonic structures modified after Navarro et al. (2009); Nunes et al. (2014); Quartau et al. (2014); Casalbore et al. (2015); and Madeira et al. (2015). Light grey area highlights submarine areas with less than 500 m water depth. Dark grey fields qualitatively show the location and orientation of major volcano-tectonic segments on Terceira, with a steeper NW-SE oriented segment, submarine along the NW Terceira Ridge and subaerial in the eastern part of Terceira, and less steep oriented segments in the western part of Terceira, intersecting Santa Bárbara volcano and Serreta Ridge (Santa Bárbara Rift). For details on the classification of Santa Bárbara Rift and Serreta units 1 and 2 as well as the tectonic segments see main text.

Submarine rock samples were taken from Serreta Ridge and the N′ Serreta Ridge SR-B (Figure. 2) using a TV-guided grab (GEOMAR Helmholtz-Zentrum für Ozeanforschung Kiel) and with a Remotely Operated Vehicle (ROV MARUM Quest 4000). Submarine samples are divided based on their sample locations considering

structural features, relative age and rock composition. Samples from the elongated eruptive centers along which the 1998–2001 Serreta eruption occurred (Gaspar et al., 2003; Casas et al., 2018; Figure 2) are considered to represent the youngest unit (unit 2). All other submarine samples are older and are summarized as unit 1, further subdivided into lavas from Serreta Ridge (SR-A) and lavas from the N′ Serreta Ridge (SR-B).

3.2. Geochemical Methods

Major element analyses for whole rocks from cruises M113 and M128 were carried out using a Spectro XEPOS He-XRF spectrometer at the GeoZentrum Nordbayern (GZN), Friedrich-Alexander-Universität (FAU) Erlangen-Nürnberg following the methods described in Romer et al. (2018). Precision and accuracy are better than 0.8% (2σ) and 1% (2σ), respectively, based on repeated measurements of the international rock standard BE-N, BR, and BHVO-1.

The major element analyses of glasses and clinopyroxenes were performed on a JEOL JXA-8200 Superprobe electron microbe at the GZN, FAU Erlangen-Nürnberg using methods and standards described in Beier et al. (2018). For glasses an acceleration voltage of 15 kV, a beam current of 15 nA, and a defocused beam (10 μm) were used. For clinopyroxene crystals the instrument was operated at 15nA, 15kV and a fully focused beam. Precision and accuracy relative to the natural volcanic glass standards VG A-99 were better than 5% (2σ) (Beier, Brandl, et al., 2018; Brandl et al., 2012) (Table S1 in the supporting information).

Major element analyses of groundmass material were performed by laser ablation ICP-MS with a NewWave UP193ss coupled to a Thermo Element2 at University of Bremen. By using a laser beam of 100 μm diameter, the major element isotopes were analyzed at high resolution. The data were quantified using the Cetac GeoPro software with USGS glass BCR-2G as external calibration standard (Jochum et al., 2005) and Ca as internal standard element; the calculated concentrations were subsequently normalized to an oxide sum of 100 wt.% with total Fe as FeO. Analytical precision and accuracy as determined by regular analyses of USGS basalt glass BHVO-2G (Jochum et al., 2005) along with the samples was <2% for most elements and <5.5% throughout (Table S3).

Trace element analyses of submarine glasses were carried out using an Agilent 7500i quadrupole ICP-MS coupled with an Analyte Excite 193nm laser (Teledyne Photon Machines) at the GZN, FAU Erlangen-Nürnberg. The trace element concentrations were determined on the same glass fragments analyzed for major element contents using the method described in Woelki et al. (2018). Ablation pattern were set to single spot analyses with 20 Hz repetition rate, 35 μm crater size in diameter and a fluence of 3 J/cm^2. Counting times were set to 20 s for background and 25 s for analysis. Accuracy was better than 15% except for Zn and Cu and reproducibility was better than 10% except for As (Table S1).

Solution trace element analyses for selected submarine whole rock samples were carried out using a Thermo Fisher Scientific X-Series 2 quadrupole ICP-MS connected to an Aridus 2 membrane desolvating sample introduction system at the GZN, FAU Erlangen-Nürnberg. For the dissolution of sample powder and rock standards (BHVO-2) we used the method described in detail in Freund et al. (2013) following standard techniques using a 3:1 mixture of HF and HNO_3. Precision and accuracy are better than 1.1% (2σ) and 1.1% (2σ), respectively, based on repeated measurements of the international rock standard BHVO-2.

New Sr-Nd-Pb-Hf isotope data from submarine samples from Serreta Ridge and N′ Serreta Ridge were processed (Sr-Nd-Pb-Hf) and analyzed (Sr-Nd-Pb) at the GZN, FAU Erlangen-Nürnberg. For Sr-Nd-Pb analysis ~150- to 200-mg dried sample powder and glasses were leached in hot 6M HCl for at least 2 h and in a 1:1:2 mixture of H_2O_2, 2.5M HCl and Milli-Q H_2O, respectively, then dissolved using the method described in Haase et al. (2017). Strontium-Nd-Hf were separated in ion-exchange columns using Biorad 50W-X8 (200–400 mesh) cationic resin with variably concentrated HCl (and HF). Neodymium was separated from Sm using LN-spec resin and the method described in Haase et al. (2017). Hafnium was separated from Ti using LN-spec resin mixture of 6M HCl+H_2O_2 and 2M HF after the method described by Hamelin et al. (2013).

Strontium and Nd isotopes were analyzed using a Thermo Fischer Triton Plus thermal ionization multicollector mass spectrometer in static mode. Strontium isotope measurements were corrected for mass fractionation using $^{88}Sr/^{86}Sr = 0.1194$, and mass 85 monitored to correct for possible contribution of ^{87}Rb to mass 87. Neodymium isotope data were corrected for mass fractionation using a $^{146}Nd/^{144}Nd$ ratio of 0.7219. Samarium interference on masses 144, 148, 150 were corrected by measuring ^{147}Sm, although the

correction was negligible for all samples presented here. During the analysis, SRM987 standard yielded $^{87}Sr/^{86}Sr = 0.710256 \pm 0.000005$, and the Erlangen Nd standard gave $^{143}Nd/^{144}Nd = 0.511543 \pm 0.000003$ (corresponding to a value of 0.511850 for the La Jolla Nd isotope standard). The data were not normalized to the measured standards.

For the digestions and Pb column chemistry only double-distilled acids were used to keep the blanks as low as possible. The separation of Pb was carried out using the method detailly described in Romer et al. (2018) using Sr-spec resin column chemistry. Lead isotope measurements were carried out on a Thermo Fisher Neptune multicollector inductively coupled plasma mass spectrometry using a $^{207}Pb/^{204}Pb$ double spike to correct for instrumental mass fractionation. Spiked and unspiked sample solutions were introduced into the plasma via a Cetac Aridus desolvating nebulizer and measured in static mode. Interference of ^{204}Hg on mass 204 was corrected by monitoring ^{202}Hg. An exponential mass fractionation correction was applied offline using the iterative method of Compston and Oversby (1969), the correction was typically 4.5 permil per amu. Twenty measurements of the NBS981 Pb isotope standard (measured as an unknown) over the course of this study gave $^{206}Pb/^{204}Pb$, $^{207}Pb/^{204}Pb$, $^{208}Pb/^{204}Pb$ ratios of 16.9410 ± 0.0020, 15.4993 ± 0.0019, and 36.7244 ± 0.0046, respectively. The Pb blanks are generally below 30 pg.

The Hf isotopes analyses for submarine samples from Serreta Ridge and N′ Serreta Ridge were carried out using a Nu Instrument Nu-Plasma II multicollector inductively coupled plasma mass spectrometry at the Bergen Geoanalytical Facility, Universitetet i Bergen, Norway. Hafnium isotopic compositions were normalized to $^{179}Hf/^{177}Hf = 0.7325$. Repeated measurements of the Ames-Grenoble Hf standard (Chauvel et al., 2011) during analyses yielded $^{177}Hf/^{176}Hf = 0.282107 \pm 0.000006$ ($n = 25$, 2σ). Hafnium isotope data are reported relative to the recommended values published by Vervoort and Blichert-Toft (1999) for JMC 475 ($^{176}Hf/^{177}Hf = 0.282160$). Standard measurements can be found in Table S2

3.3. Clinopyroxene-Melt Thermobarometry

Euhedral clinopyroxenes in textural equilibrium with the host melt (glass or groundmass) of 12 basaltic samples were selected for clinopyroxene-melt thermobarometry. The host melt compositions were determined by glass analyses using electron microprobe, or by LA-ICP-MS analyses of groundmass if the samples were not glassy or the glass contained abundant microliths (Table S3). Clinopyroxene rim composition were determined by six to eight single point analyses at 5- to 10-μm distance from the rims by electron microprobe, which reflect the conditions of last equilibrium between crystal and melt. For most clinopyroxene-host melt pairs the thermobarometer calibrations by equations A and B of Table 4 of Putirka et al. (2003) were used, which provide the most precise estimates (Putirka, 2008). They have a standard error of estimate of ±33°C and ±1.7 kbar, although estimates can be more precise if a number of analyses are used and averaged (Putirka et al., 2003). For three trachytic samples from the subaerial Santa Bárbara volcano the thermobarometer calibrations Palk2012 and Talk2012 of Masotta et al. (2013) were applied instead, which for highly evolved alkalic melts performs better than the Putirka et al. (2003) calibrations.

The clinopyroxene-melt pairs were tested for chemical equilibrium by applying the following filters: (1) the equilibrium constant for Fe-Mg exchange $K_D^{Fe\text{-}Mg}$ is within 0.28 ± 0.08 (Putirka, 2008) and (2) the calculated clinopyroxene components DiHd, EnFs, CaTs, and Jd are within $\pm 2\sigma$ of the values predicted by the Putirka (1999) model. For trachytes the observed $K_D^{Fe\text{-}Mg}$ had to agree with the value predicted by eq. (35alk) of Masotta et al. (2013). All clinopyroxene-melt pairs failing any of these criteria (210 of 477 measured) and those yielding negative pressures were discarded. A further assessment of chemical equilibrium is provided by the clinopyroxene Al content normalized to six oxygens, which for all analyses is above the equilibrium threshold of 0.11 (Neave & Putirka, 2017).

4. Results

4.1. Bathymetry and Orientation of Volcanic Structures

West of Terceira, the Serreta Ridge and the NW Terceira Ridge form two major volcanic structures that rise up to 2500 m above the surrounding seafloor extending from the island into the Eastern Graciosa Basin (Quartau et al., 2014; Figure 2). Both ridges are narrow and consist of several aligned volcanic cones, lava flows and elongated eruptive centers (Casalbore et al., 2015; Chiocci et al., 2013; Quartau et al., 2014). Serreta Ridge has an along axis length of ~25 km and extends from the Santa Bárbara volcano in WNW

direction. The NW Terceira Ridge has a NW-SE orientation with elongated eruptive centers striking in ~140° direction (Casalbore et al., 2015), in contrast to those from Serreta Ridge striking ~120°. Smaller volcanic ridges with elongated volcanic centers forming SR-B and SR-C of the N′ Serreta Ridges (Figure 2) are located between the Serreta and Northwest Terceira Ridges. Their strike direction is relatively variable between 135° and 170° (Casalbore et al., 2015; Figure 2). Elongated eruptive centers that are oriented different to those at Serreta Ridge also occur south of Serreta Ridge [striking between 65° and 90°; Figure 2; Casalbore et al., 2015]; however, volcanic structures related to the magmatism offshore Terceira are much more common north of Serreta Ridge. The ridges and elongated eruptive centers west of Terceira (excluding the NW Terceira Ridge) form a radial arrangement around the subaerial Santa Bárbara volcano, with Serreta Ridge as the most pronounced submarine structure.

Subaerially, volcano-tectonic structures in the western part of Terceira are also oriented radially around a common center that seems to be located at the caldera of the Santa Bárbara volcano and these structural features continue into the offshore environment (Figure 2). Structures located subaerially in the extension of the Serreta Ridge form the most pronounced subaerial volcano-tectonic structures in the western part of Terceira. Alignments of volcanic cones ESE of the Santa Bárbara caldera are oriented between 110 and 120° strike (Pimentel et al., 2016), equivalent to similarly oriented structures WNW of Santa Bárbara (Madeira et al., 2015), and Serreta Ridge (Casalbore et al., 2015). The area in which subaerial and submarine volcano-tectonic structures are predominantly oriented WNW-ESE is therefore summarized as Santa Bárbara Rift.

4.2. Major and Trace Element Geochemistry

Published data for the volcanic rocks from the subaerial Santa Bárbara volcano (see Figure 3 for references) and the new data from the submarine Serreta Ridge and N′ Serreta Ridge range from alkali basalts to trachytes and thus cover the entire range from mafic to highly evolved rock composition (Figure 3). Lavas from the submarine fissure zones are mafic to intermediate in composition ranging from 12.9 to 4.6 wt.% MgO and 45 to 48 wt.% SiO_2, respectively. In contrast, lavas from the subaerial Santa Bárbara central volcano are intermediate to highly evolved rocks with MgO from 4.6 to 0.1 wt.% and SiO_2 from 47 to 70 wt.% (Figure 3). Glass and groundmass analyses from the submarine fissure zones have a notably smaller range in MgO than the whole rocks and lie between 7.1 and 4.6 wt.%. The primitive Terceira melts have been interpreted to have a MgO content ≥8 wt.% (Madureira et al., 2011), however, lavas >12.5 wt.% MgO are likely the result of the accumulation of clinopyroxene and olivine (Beier et al., 2008). Subaerial lavas from fissure zones display the largest variability with 12 to <0.5 wt.% MgO, but the majority of these lavas have a MgO content >5 wt.%, similar to the submarine lavas.

The submarine lavas cover a relatively large range in major elements, for example, ranging from 2.0–3.5 wt.% TiO_2 and 8.5–12.0 wt.% FeO^T, respectively, at a given MgO content of ~7 wt.% (Figure 3). Lavas from unit 2, which are partly associated with the 1998–-2001 Serreta eruption, tend toward the lowest TiO_2, FeO^T, Na_2O, and K_2O and highest SiO_2 and CaO contents.

Similarly, lavas from unit 2 have the highest Ba/Nb, Lu/Hf and lowest La/Yb and Nb/U (Figure 4). Lavas from unit 1 have a larger range in major elements and trace element ratios than unit 2, irrespective of whether they are from Serreta Ridge or the N′ Serreta Ridge (Figure 4). Subaerial lavas from the W′ fissure zone with MgO >4 wt.% have compositions similar to submarine lavas. In contrast, lavas from the main fissure zone are chemically different from all other volcanic units in that they display Ba/Nb and La/Yb ratios of 8–15 and 12–18 at given MgO contents >5 wt.%, compared to 5.0–7.5 and 10–14 for the submarine lavas.

4.3. Isotope Geochemistry

The radiogenic Sr-Nd-Pb-Hf isotope ratios show significant variations between the different subaerial and submarine units (Figure 5). In general, lavas from subaerial and submarine fissure zone as well as from the Santa Bárbara volcano are within the range of lavas from the central Azores [Faial, Pico, São Jorge and Graciosa; Elliott et al., 2007; Beier et al., 2008; Hildenbrand et al., 2008; Millet et al., 2009; Beier et al., 2012; Hildenbrand et al., 2014; Larrea et al., 2014; Béguelin et al., 2017; Beier, Haase, & Brandl, 2018; Romer et al., 2018], for example, ranging from 19.7 to 20.1 and from 0.70345 to 0.70364 in $^{206}Pb/^{204}Pb$ and $^{87}Sr/^{86}Sr$, respectively. The only exception are some lavas from Terceira's main fissure zone which have less radiogenic Pb and Sr isotope ratios ranging from 19.3 to 19.7 and 0.7033 and 0.7035 in $^{206}Pb/^{204}Pb$ and $^{87}Sr/^{86}Sr$ ratios, respectively (Figure 5).

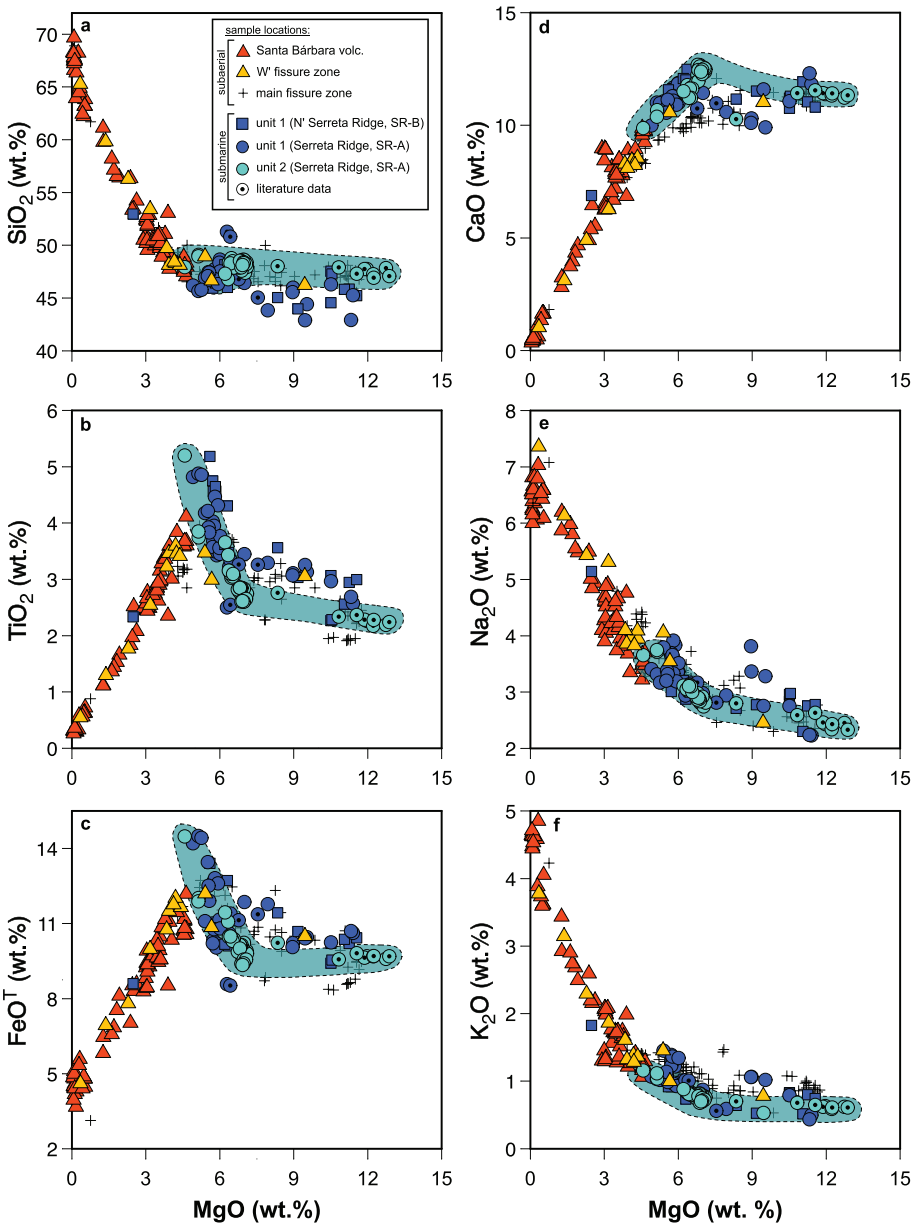

Figure 3. (a) SiO_2, (b) TiO_2, (c) FeO^T, (d) CaO, (e) Na_2O, and (f) K_2O versus MgO contents of submarine Serreta and N' Serreta Ridge and subaerial Terceira lavas. Bright blue fields highlight the lavas from the youngest volcanic eruptive fissure at Serreta Ridge (unit 2) along which the 1998–2001 Serreta eruption occurred. Subaerial data from Terceira are from Beier et al. (2008); Madureira et al. (2011); Hildenbrand et al. (2014); Zanon and Pimentel (2015) and Pimentel et al. (2016). Submarine literature data are marked with a black dot and are from Zanon and Pimentel (2015) and Madureira et al. (2017).

Other lavas from Terceira and its submarine fissure zones can be further distinguished based on their isotope geochemistry. Submarine lavas from unit 1 have more radiogenic Pb isotope ratios compared to unit 2 lavas, but similar Sr and Nd isotope ratios. Lavas from unit 1 have $^{206}Pb/^{204}Pb$ and $^{208}Pb/^{204}Pb$ of 19.94–20.02 and 39.25–39.39 compared to 19.73–19.86 and 39.12–39.16 for unit 2 lavas. One single sample of unit 1 (IEAZO0995) is within the range of unit 2 lavas for $^{206}Pb/^{204}Pb$, but is different in $^{208}Pb/^{204}Pb$, $^{87}Sr/^{86}Sr$ and $^{176}Hf/^{177}Hf$. The $^{176}Hf/^{177}Hf$ ratios of unit 1 lavas are relatively variable ranging from ~0.28302 to ~0.28316 and overlap with lavas from unit 2. There is, however, a broad negative correlation in Hf-Pb isotope space with unit 1 lavas trending toward more radiogenic Pb and lower $^{176}Hf/^{177}Hf$ (Figure 5). Subaerial lavas

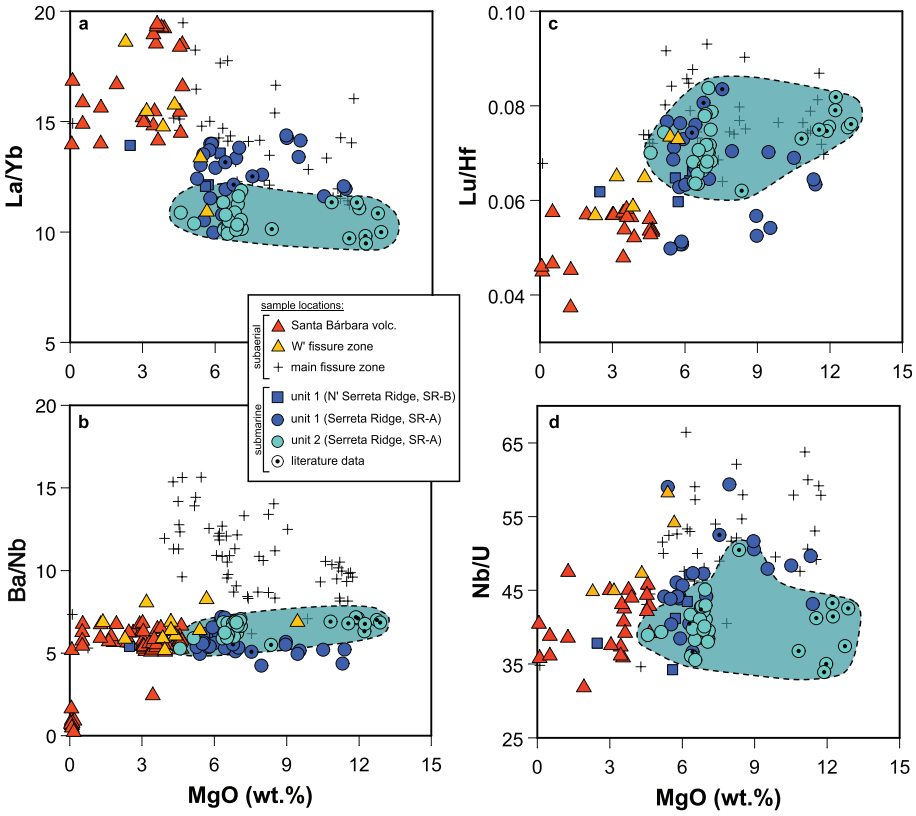

Figure 4. (a) La/Yb, (b) Ba/Nb, (c) Lu/Hf, and (d) Nb/U ratios versus MgO contents. Data sources are the same as in Figure 3.

from Santa Bárbara volcano and the W' fissure zone overlap with lavas from unit 1 in all radiogenic isotope ratios considered here. They are, however, distinct from unit 2 lavas in $^{206}Pb/^{204}Pb$ and $^{208}Pb/^{204}Pb$ ratios and the majority also tends to lower $^{176}Hf/^{177}Hf$.

4.4. Thermobarometry

The clinopyroxene-melt thermobarometry for the submarine lavas shows a wide range of pressures from around ~0 to 8.9 kbar, with a well-defined frequency maximum at 6.25–6.75 kbar (Figure 6). This frequency maximum is similar for both units 1 and 2 but also for Serreta Ridge and the N' Serreta Ridge (both unit 1). The results overlap with fluid inclusion data from the 1998–2001 Serreta eruption, which indicate a maximum pressure at 5.75 kbar (Zanon & Pimentel, 2015). As the depth to the Moho is inferred to be at around 18–20 km based on fluid inclusion and geophysical studies (Spieker et al., 2018; Zanon & Pimentel, 2015), equivalent to about 5.0–5.5 kbar, our data indicate that pre-eruptive magma storage and crystal fractionation occur in the uppermost mantle (Figure 6). In contrast to the fluid inclusion studies from Zanon and Pimentel (2015) our submarine data displays subordinately lower pressures down to ~0.3 kbar and ~2.5 kbar for unit 1 and unit 2, respectively. In contrast to unit 1, unit 2 lavas display a subordinate frequency maximum near the Moho around 5 kbar, and the maximum at 6.25–6.75 kbar is less pronounced.

Temperatures obtained by clinopyroxene-melt thermometry reveal some differences between unit 1 and unit 2 lavas. Temperatures for unit 1 range from 1133 to 1218°C with a mean of 1184 ± 17°C and a median of 1184°C (Figure 6). The frequency maximum for unit 1 is similarly well-defined for both Serreta Ridge and N' Serreta Ridge. Unit 2 displays a narrower range and higher temperatures from 1181 to 1231°C with a mean of 1208 ± 10°C and a median of 1211°C.

The clinopyroxene-melt thermobarometry on the evolved Santa Bárbara lavas results in significantly lower pressures and temperatures compared to the basaltic submarine and subaerial lavas from the fissure zones (Zanon & Pimentel, 2015). Pressures and temperatures for Santa Bárbara lavas are well-defined with a range

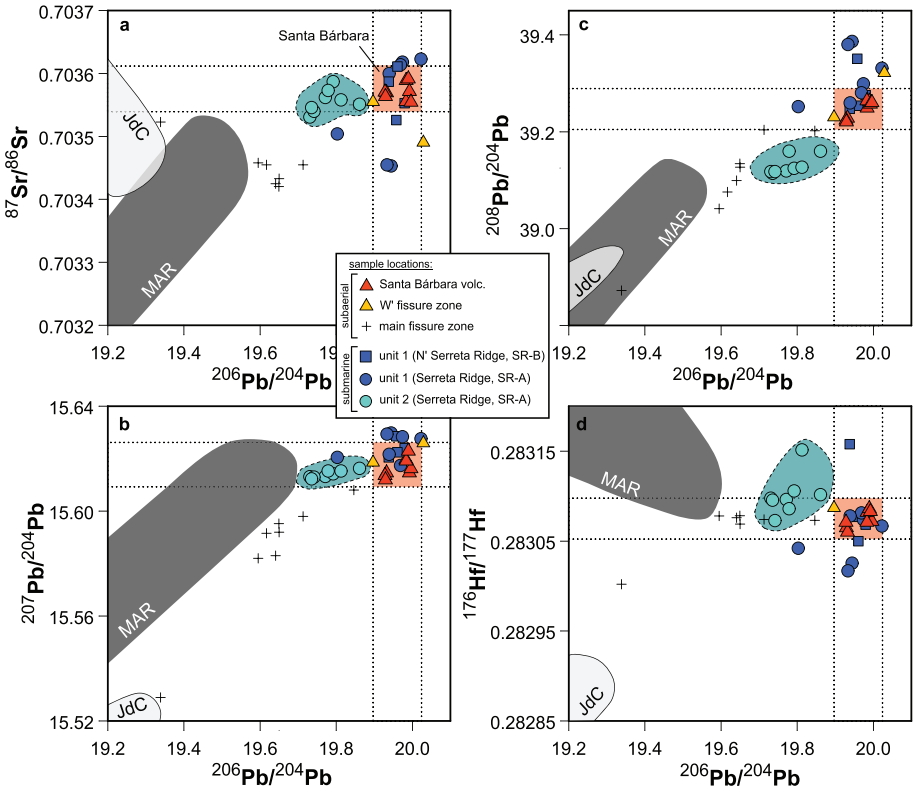

Figure 5. (a–d) Sr-Pb-Hf isotope ratios of submarine and subaerial lavas from Terceira. Areas highlighted in bright and dark grey are background reference data from the D. João de Castro seamount (Béguelin et al., 2017; Beier et al., 2008) and the MAR (Agranier et al., 2005; Dosso et al., 1999; Gale et al., 2011; Gale et al., 2013; Hamelin et al., 2013; Shirey et al., 1987). Red rectangles highlight the isotopic range of Santa Bárbara volcano. Data sources of Terceira samples are the same as in Figure 3 with additional data from Béguelin et al. (2017).

from 843 to 862°C and 0.64 to 1.3 kbar, respectively (Figure 6). The temperatures for Santa Bárbara overlap with the temperature range for peralkaline felsic volcanism of Terceira of 773–936°C from Jeffery and Gertisser (2018), which were derived from studies of the neighboring Pico Alto volcano (D'Oriano et al., 2017; Jeffery et al., 2017).

5. Discussion

5.1. Chemical and Structural Segmentation

Subaerial lavas from Terceira are separated into those erupting from central volcanoes and those from the fissure zones (Self & Gunn, 1976). Distinct mantle sources involved in the formation of lavas from subaerial and submarine fissure zones and central volcanoes may be used as tracers for magma transport through the crust. The source composition of lavas from related volcanic units are highly variable indicating mantle source heterogeneity on a small spatial scale (Madureira et al., 2011) similar to other Azorean islands (Béguelin et al., 2017; Beier, Haase, & Brandl, 2018). Notably higher Ba/Nb and Nb/U and less radiogenic Pb isotope ratios of lavas from the main fissure zone compared to lavas from Santa Bárbara volcano are interpreted to result from different mantle source compositions. Lead-Hf isotope ratios, most trace element ratios (Figure 7) and recent studies by Madureira et al. (2011) and Béguelin et al. (2017) show that these lavas are influenced by a low Pb and Hf mantle source endmember. In contrast to main fissure zone, submarine lavas and from the subaerial W' fissure zone (Figure 2) have Ba/Nb and Nb/U overlapping with Santa Bárbara lavas at comparably radiogenic $^{206}Pb/^{204}Pb$, $^{207}Pb/^{204}Pb$, and $^{208}Pb/^{204}Pb$ ratios (Figure 7). Thus, generally, lavas from the submarine fissure zone and the W' fissure zone have a mantle source composition comparable to Santa Bárbara, indicating that they are genetically linked, independent of whether lavas derive from a volcanic fissure zone or the central volcano.

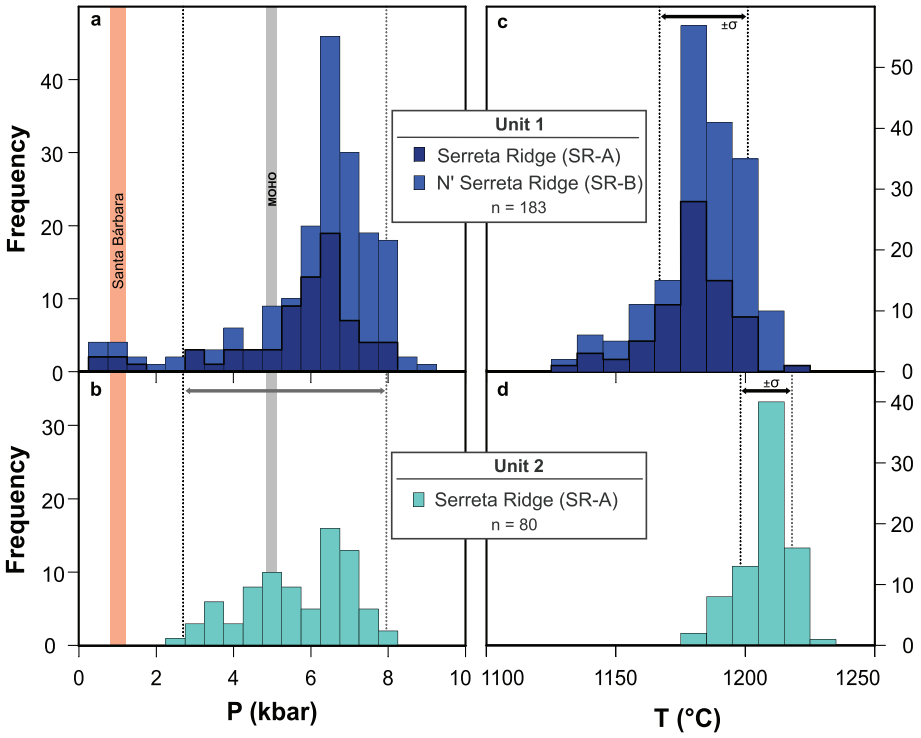

Figure 6. (a and c) Pressures (P) and (b and d) temperatures (T) of selected submarine lavas from Serreta Ridge and the N' Serreta Ridge (cf. Figure 2) from clinopyroxene-melt thermobarometry versus their frequency of occurrence (bin size is 0.5 kbar and 10°C, respectively). Lavas from unit 1 are subdivided into whether they derive from Serreta Ridge or the N' Serreta Ridge. The dotted lines in (a, unit 1) and (b; unit 2) display 90% of all crystallization pressures (between 2.70 and 7.96 kbar). The dotted lines in (c; unit 1) and (d; unit 2) mark the ±σ on the means of 1184 °C (unit 1) and 1208 °C (unit 2). The grey bar in (a) and (b) marks the location of the Moho beneath Terceira, inferred to be located at ~18-km depth (Spieker et al., 2018). Red bar in (a) and (c) highlight the pressure range of Santa Bárbara lavas from clinopyroxene-melt thermobarometry (see details in the text).

Volcanic cones of the main fissure zone, like, for example, those immediate north and east of the W' fissure zone, erupted geochemically and petrologically distinct lavas. These are interpreted to derive from different plumbing systems but have similar ages [<10 ka; Zanon & Pimentel, 2015], showing that melt transport through the mantle and crust preserves source differences on a small spatial and temporal scale. This has been shown in previous studies from Pimentel et al. (2016) on the basis of two neighboring volcanic systems, the Mistérios Negros (W' fissure zone) and the CE 1971 lava flow (main fissure zone) situated <2-km distance from each other. More importantly, these data show that the fissure zones (<50 ka; in the example above <10 ka) and Santa Bárbara (<65 ka) volcano are active contemporaneously (Madureira et al., 2011; Pimentel et al., 2016; Self, 1976), suggesting that the variability of mantle source compositions is spatial rather than temporal in nature. We note, however, that only four isotope data from the eastern and older central volcanoes Cinco Picos, Guilherme Moniz and Pico Alto are available. The available samples have relatively low Ba/Nb ratios between 6 and 9, thus, they do not cover the entire compositional range of 4 to 13 of the island (Figure 7). Hence, it remains to be tested if the eastern central volcanoes are isotopically similar to the main fissure zone. We conclude, that lavas from Santa Bárbara volcano, the W' fissure zone and the submarine fissure zones (Santa Bárbara Rift) are derived from a different mantle source than those from the main fissure zone.

These differences in mantle source composition chemically divide the island into an eastern and western part (Figure 7) in the younger volcanic history of <65 ka. This chemical segmentation is in agreement with a segmentation of the volcano-tectonic structures in the eastern and western part of Terceira (cf. Figure 2c). The predominant WNW-ESE orientation of the Santa Bárbara Rift (consisting of the W' fissure zone, Serreta Ridge and the Santa Bárbara volcano; Figure 2), is accompanied by the distinct mantle source of the western

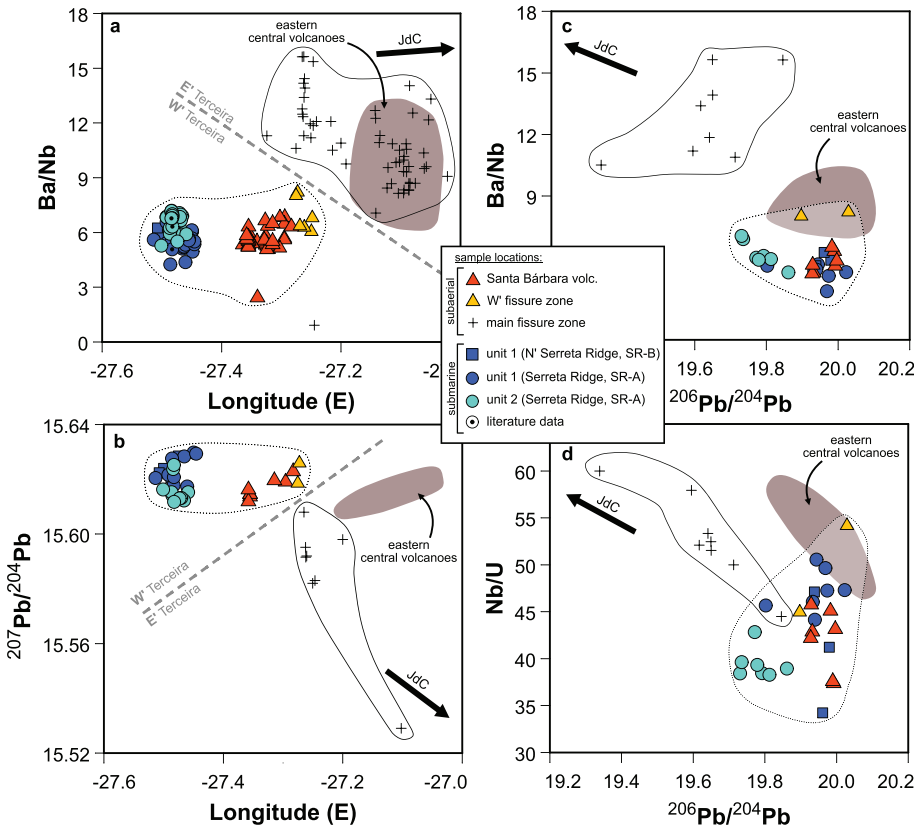

Figure 7. Longitude (E) versus (a) Ba/Nb and (b) $^{207}Pb/^{204}Pb$ ratios and $^{206}Pb/^{204}Pb$ versus (c) Ba/Nb and (d) Nb/U ratios for all submarine and subaerial Terceira lavas >3 wt.% MgO (a, c, and d). Lavas erupted in the eastern part of Terceira along predominantly NW-SE oriented structures are chemically distinct to lavas from the western part of Terceira erupted along WNW-ESE oriented structures. Fields with a dotted line highlight lavas from the Santa Bárbara Rift; fields with solid line highlight lavas from the main fissure zone. Brown field additionally highlights literature data of the central volcanoes located in the eastern part of Terceira from Beier et al. (2008) and Hildenbrand et al. (2014). The black arrow indicates the trace element and isotope signature of D. João de Castro (JdC) seamount based on data from Beier et al. (2008) and Béguelin et al. (2017). Data sources are the same as in Figure 5.

Terceira magmatic system (Figure 7). However, small-scale mantle source heterogeneities still exist underneath the western part of Terceira, the implications of which will discussed below. In contrast to the western part of Terceira, structural features in the eastern part of Terceira (eastern central volcanoes and the main fissure zone) are dominated by NW-SE oriented structural features coherent with the orientation of the Lajes graben (Madeira et al., 2015; Marques et al., 2015; Navarro et al., 2009; Nunes et al., 2014). This NW-SE orientation is accompanied by the distinct mantle source signature of the main fissure zone, which has been shown to be influenced by the D. João de Castro seamount mantle sources located ~60 km SE of Terceira (Madureira et al., 2011; Béguelin et al., 2017; Figure 7).

We conclude that the western and eastern part of Terceira are situated on a tectonically defined segment (Lourenço et al., 1998), respectively, each with distinct magma compositions. We find no obvious evidence for large scale magma or source mixing between the segments. We will discuss below whether and how the volcanic activity of Santa Bárbara volcano and the western submarine and subaerial fissure zones are linked considering that these systems are genetically decoupled from eastern Terceira.

5.2. Chemical Variation in the Western Terceira Magmatic System

Crustal melt transport via sills and dikes generally favors tectonic pathways in the crust, that is, for the specific case of Serreta Ridge, magma transport will occur as a result of the WSW-ENE transtensional stresses (Neves et al., 2013). Based on the structures, Serreta Ridge and the N' Serreta Ridges can be separated into several subparallel segments, reflecting several focused volcanic eruptions (Figure 2). It is common for

single eruptions to emit from several segments of an en-échelon fissure (Klügel, Walter, et al., 2005). Lavas from the different segments, however, also differ in composition, suggesting that different segments represent different volcanic eruptions.

At a given MgO content lavas from unit 1 comprise a larger variability in major and trace element composition compared to the younger unit 2 (Figures 3 and 4). Despite of larger chemical variability of unit 1, lavas from the youngest part of Serreta Ridge (unit 2) display the most depleted source signature. In agreement with the highest SiO_2, CaO and lowest TiO_2, FeO^T, and K_2O contents of unit 2 relative to unit 1, incompatible trace element ratios such as Ba/Nb and Lu/Hf are highest and Nb/U and La/Yb are lowest (at a given MgO content of >5 wt.%). Lower La/Yb ratios additionally indicate that lavas from unit 2 may have originated from a higher degree of partial melting than unit 1 lavas (Bourdon et al., 2005). We note, however, that the degree of partial melting and the mantle source composition may be linked, that is, differences in trace element ratios such as La/Yb may result from both, different degrees of enrichment in the mantle source and changes in degree of partial melting (Haase et al., 2011).

Unit 1 isotopically resembles lavas from Santa Bárbara and the W′ fissure zone, suggesting a connection to a common magma plumbing system. Lavas from the N′ Serreta Ridge resemble those from Serreta Ridge unit 1, indicating that they may have originated from similar mantle source and plumbing system, although they are located on distinct and differently oriented ridges. The chemically distinct character of unit 2, which is the youngest lava suite, indicates that melts erupted at Serreta Ridge display a progressive change in composition with age.

5.3. Ponding Depth and the Role of Fractional Crystallization

Previous studies have shown that lavas from Terceira display a bimodal distribution of lava compositions (Mungall & Martin, 1995; Self, 1976). Santa Bárbara and the other central volcanoes erupt intermediate to highly evolved rocks (<5 wt.% MgO), whereas those erupted from the subaerial and submarine fissure zones are mafic to intermediate in composition (<12 wt.% MgO; Figure 3). Thus, lavas from the subaerial and submarine fissure zones experience less extensive fractional crystallization during their ascent than those from Santa Bárbara. This implies that Santa Bárbara volcano has a well-established shallow crustal magmatic system where extensive (50–-65%) crystal fractionation occurs which led to explosive volcanic activity in the past and the formation of a caldera ~15 ka ago (Larrea et al., 2018; Madureira et al., 2011; Mungall & Martin, 1995). The fissure zone magmas, on the other hand, are more primitive and may ascend directly from deeper and more mafic levels of the magma system, bypassing the shallower reservoir.

Mineral thermobarometry is useful to define stagnation levels of ascending magmas in the mantle and crust and allows to refine the implications arising from changes in melt movement at crustal levels. High pressures of ~5 and ~6 to 7 kbar around and beneath the Moho, respectively, dominate the submarine lavas from Serreta Ridge and N′ Serreta Ridge (Figure 6) as well as from subaerial fissure zones [maximum at 4.98 kbar; Zanon & Pimentel, 2015], and are in agreement with the relatively low degree of fractionation. Moho and sub-Moho depths are common levels of stagnation in ocean islands (Klügel et al., 2015; Klügel, Hansteen, & Galipp, 2005; Zanon & Frezzotti, 2013; Zanon & Pimentel, 2015). The highest pressures for the Serreta lavas are at ~ 7 kbar, which is higher than those from Zanon and Pimentel (2015) based on fluid-inclusion thermobarometry (maximum at 5.75 kbar), and can be explained by the different response rates of fluid-inclusion and clinopyroxene-melt barometers (Klügel et al., 2015).

Jeffery and Gertisser (2018) have shown that peralkaline intraplate volcanoes from the Atlantic Ocean commonly have a magma reservoir in 2- to 5-km depth, where melts fractionate to trachytic compositions. The base of a central volcanoes is a common upper crustal level for stagnation of ascending magmas, where sedimentary layers and the volcanic edifice have lower densities (Klügel, Hansteen, & Galipp, 2005). For the specific case of the Azores we consider the presence of large quantities of sediments unlikely due to the young age and limited quantity of sediments however, the igneous lithologies may act as a density barrier. Other central volcanoes in the Azores, for example, the neighboring Pico Alto volcano (Jeffery et al., 2017), Sete Cidades (Beier et al., 2006) and Furnas (Jeffery et al., 2016) on São Miguel, and the Caldeira volcano on Faial (Dias et al., 2007) also have shallow magma reservoirs in 2- to 4-km depth (3–7 km for the Caldeira volcano) and our barometric data for Santa Bárbara agree with these observations.

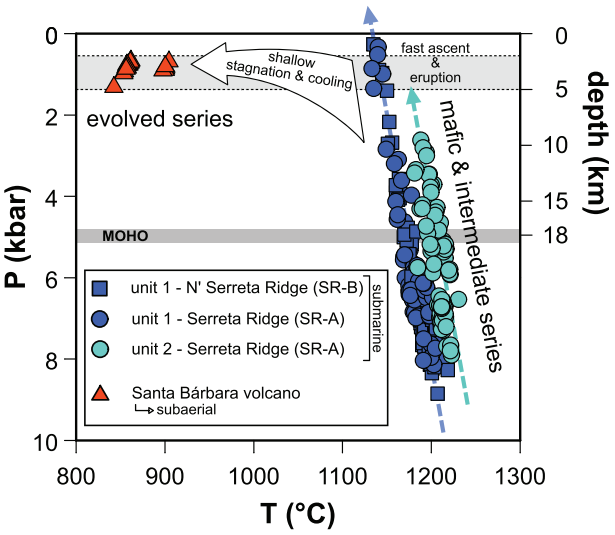

Figure 8. Pressures (P) versus temperatures (T) from clinopyroxene-melt thermobarometry for submarine units 1 and 2 as well as for subaerial lavas from Santa Bárbara grouped based on classification used in Figure 3. Bright and dark blue arrows indicate the P-T conditions of units 1 and 2 during magma ascent. Note that lavas from unit 2 display higher temperatures compared to lavas from unit 1. The temperature differences between mafic to intermediate submarine and evolved Santa Bárbara lavas indicate that extensive fractional crystallization occurs predominantly at very shallow stagnation levels. The lack of higher pressures for the Santa Bárbara lavas indicates that melts feeding submarine fissure eruptions may also have replenished the shallow Santa Bárbara magmatic system. Dark grey bar shows the pressure range for the Moho beneath Terceira from Spieker et al. (2018). The light grey field highlights the depth range for shallow magma reservoirs for Pico Alto volcano (and Guilherme Moniz volcano) on Terceira (Jeffery et al., 2017; Jeffery & Gertisser, 2018), which is similar to the typical depth range for peralkaline magmas in crustal reservoirs of Atlantic Ocean islands in general (Jeffery & Gertisser, 2018). The depth (km) refers to the crust beneath Serreta Ridge based on a density of 2800 kg/m^3 (Zanon & Pimentel, 2015).

Using a density of 2500 kg/m^3 for the crust beneath Terceira based on Zanon and Pimentel (2015), the obtained pressures of 0.6- to 1.3-kbar result in a depth of 2.6 to 5.2 km for Santa Bárbara volcano. This is in agreement with the depth for the base of the central volcanoes beneath Terceira of ~2 km based on seismic studies from Spieker et al. (2018).

We thus conclude that the highly evolved rock compositions from Santa Bárbara indicate that stagnation and fractional crystallization in upper (<5-km depth) crustal levels is a major process in the evolution of the central volcano. Santa Bárbara thus represents a mature stage in the evolution of a oceanic intraplate volcano (Klügel et al., 2015) with a more complex plumbing system compared to the generally mafic lavas from the fissure zones.

5.4. Implications on the Melt Transport in the Western Terceira Magmatic System

5.4.1. Link Between Santa Bárbara and Serreta Ridge

The strong structural connection, similar isotopic signatures and thermobarometric results (Figures 2, 5, and 8) indicate that unit 1 and Santa Bárbara share a common plumbing system at depth and are laterally transported from the deeper plumbing system located beneath Santa Bárbara volcano to the Serreta Ridge. This is also supported by studies on fossil flow patterns from dykes on the Azorean islands (e.g., São Miguel and Santa Maria), indicating that melts generally propagate away from a volcanic center (Moreira et al., 2015).

Studies on Iceland (e.g., Gudmundsson, 2000), Hawaii (e.g., Garcia et al., 1996) and Fernandina Island (Geist et al., 2006) show that dyke swarms are often fed laterally from a shallow crustal magma reservoir beneath a central volcano. A possible mechanism driving the emplacement and flow direction of dykes is a topographic gradient between the shallow reservoir and the eruptive site. This can be observed at Krafla volcano on Iceland, where a shallow magma reservoir located at ~3-km depth feeds dykes migrating in NNW direction while increasing in dyke depth (Hollingsworth et al., 2012). Similarly, melt transport from the central volcano on Fernandina Island (Galápagos) into submarine fissure zones occurs very shallow in 1.5-km depth at comparable crustal and lithospheric thicknesses compared to Terceira (Geist et al., 2006; Gibson & Geist, 2010). The bimodal distribution in the degree of fractionation between Santa Bárbara and the corresponding fissure zones shows that magmas erupted from Santa Bárbara have stagnated and fractionated in a shallow magma reservoir, which is however bypassed by magmas erupted from the fissure zones. There is no petrological or geochemical evidence such as magma mixing or felsic xenoliths that the mafic to intermediate Serreta magmas have interacted with highly evolved melts from Santa Bárbara. Thus, the lateral transport of melts from the Santa Bárbara plumbing system into the fissure zones must occur at depths greater than the levels at which extensive fractional crystallization occurs (>5 km; Figure 8). The predominant occurrence of Moho and mantle pressures at the volcanic fissure zones rule out prolonged upper crustal residence and ascent. Extensive fractional crystallization is absence in the uppermost crust at Fernandina Island with SiO_2 contents of erupted lavas that do not exceed 52 wt.% (Geist et al., 1995). Thus, lateral melt transport at Fernandina Island occurs at shallower crustal levels compared to the Santa Bárbara magmatic system which we interpret to result from the stronger structural regime in the Azores and more evolved melts in the shallow crust compared to the Galápagos islands. We note, that the presence of more evolved melts beneath Santa Bárbara is related to differences in the magmatic production between these systems, which is notably higher at Galápagos compared to the Azores (Mjelde et al., 2010).

Similar to lavas from unit 1, the fissure zones between Santa Bárbara and Pico Alto volcanoes also display ponding at shallower crustal levels [~8.5-km depth; Zanon & Pimentel, 2015]. These are interpreted to reflect stagnation at intra-crustal magmatic bodies related to the plumbing systems of Santa Bárbara volcano, acting

as density barrier for ascending melts. We conclude that lateral melt transport along the fissure zones occur within the lower crust to Moho depths over tens of kilometers.

5.4.2. Direction of Melt Transport

The predominant WNW-ESE orientation of volcano-tectonic structures along the Santa Bárbara Rift indicates that lateral melt transport occurs predominantly in WNW and ESE directions. Because dykes as hydrofractures are mostly oriented perpendicular to the least compressive stress σ_3 (Anderson, 1951) the NNE-SSW directed opening of the Terceira Rift at the western part of Terceira explains the WNW-ESE oriented volcanic and tectonic structures and follow the regional tectonic stress field (Pimentel et al., 2016). In contrast, radially oriented volcano-tectonic structures around a common center are known from dyke injections from a shallow magma reservoir of a volcanic edifice (Burchardt et al., 2018), for example, at the central volcano of Fernandina Island (Chadwick & Dieterich, 1995) and associated radially oriented submarine fissure zones (Geist et al., 2006). Some subaerial structures around Santa Bárbara volcano and submarine structures at the N' Serreta Ridges and south of Serreta Ridge are oriented radially around Santa Bárbara caldera (Figure 2). These structures are influenced by local volcanotectonic and gravitational stresses derived from the magma reservoir beneath Santa Bárbara volcano. Indeed, several known volcanic systems combine structural features from both regional and local stresses in subcircular edifices like Santa Bárbara, for example, Mt. Etna, Italy (Acocella & Neri, 2009; McGuire & Pullen, 1989). Thus, whereas most dominant volcano-tectonic structures around Santa Bárbara volcano reflect melt movement along the rift in WNW and ESE directions, local stresses force magma pathways distributed radially around the Santa Bárbara caldera (Figure 9).

The lateral extent of submarine volcanic activity at the Serreta Ridge related to the Santa Bárbara volcano is much larger (~25 km) than the subaerial W' fissure zone with a 5 km along axis distance (Figure 9). Thus, lateral melt transport from the Santa Bárbara plumbing system is asymmetric and preferentially occurs in WNW direction, whereas ESE melt transport seems to be of subordinate importance. This asymmetry may be the result of the abundant crustal intrusions beneath Terceira. Crustal intrusive complexes feeding the central volcanoes hamper the ascent and transport of melts in the crust beneath Terceira (Zanon & Pimentel, 2015). The crust beneath Terceira is warm with an estimated bulk density of around 2500 kg/m^3, significantly lower than 2,800 kg/m^3 for the crust beneath Serreta Ridge (Zanon & Pimentel, 2015). Both the low density and elevated temperatures are an obstacle for propagating mafic dykes (Menand, 2011) and can result in dyke arrest or deflection and lateral propagation. In addition to pre-existing crustal intrusions, the observed asymmetry in dyke distribution may reflect the influence of local gravitational stress from the topographic load of the Terceira central volcanoes, which superimposes the regional tectonic stress field (McGuire & Pullen, 1989). It is a common observation that seamounts and volcanic islands develop radiating submarine ridges during their growth (Mitchell, 2001).

5.4.3. New Mantle Magma Pulse at Serreta Ridge

The Serreta Ridge is fed by two independent magmatic systems with distinct mantle source compositions. Lavas from unit 2 are not linked to Santa Bárbara volcano, in contrast to unit 1 lavas (Figure 6), implying that the compositional variability in the different units along Serreta Ridge occurs on a very small spatial scale (distance between the eruptive fissures is <2 km). Thus, Serreta Ridge does not form one single volcanic unit, but reflects the evolution of at least two magmatic system. It is however unclear which factors control how melts ascend and interact in the crust beneath Serreta, that is, why lavas from unit 1 are similar and lavas from unit 2 are distinct compared to Santa Bárbara lavas.

The tectonic stress field prevailing in the Azores is a major controlling factor on the pathways and ascent of melts and on the morphology and orientation of volcanic bodies. This has been shown to be the case for most Azorean islands (e.g., Madeira et al., 2015) and other tectonically influenced settings, for example, in Iceland (Gudmundsson, 2000). Another controlling factor for volcano distribution at these systems are processes in the mantle. Magmatism along the Terceira Rift indicates focused melt ascent beneath the islands and seamounts, whereas areas in between the islands are generally volcanically inactive (Beier et al., 2008). These observations are consistent with distinct mantle source compositions for each island/seamount with limited evidence of mixing between the magmatically active segments. On most islands in the Eastern Azores the occurrence of central volcanoes/volcanic centers is characterized by a progressive age propagation from east to west (Calvert et al., 2006; Feraud et al., 1980; Hildenbrand et al., 2008; Hildenbrand et al., 2012; Hildenbrand et al., 2014; Johnson et al., 1998; Larrea et al., 2018; Quartau et al., 2014) indicating that the

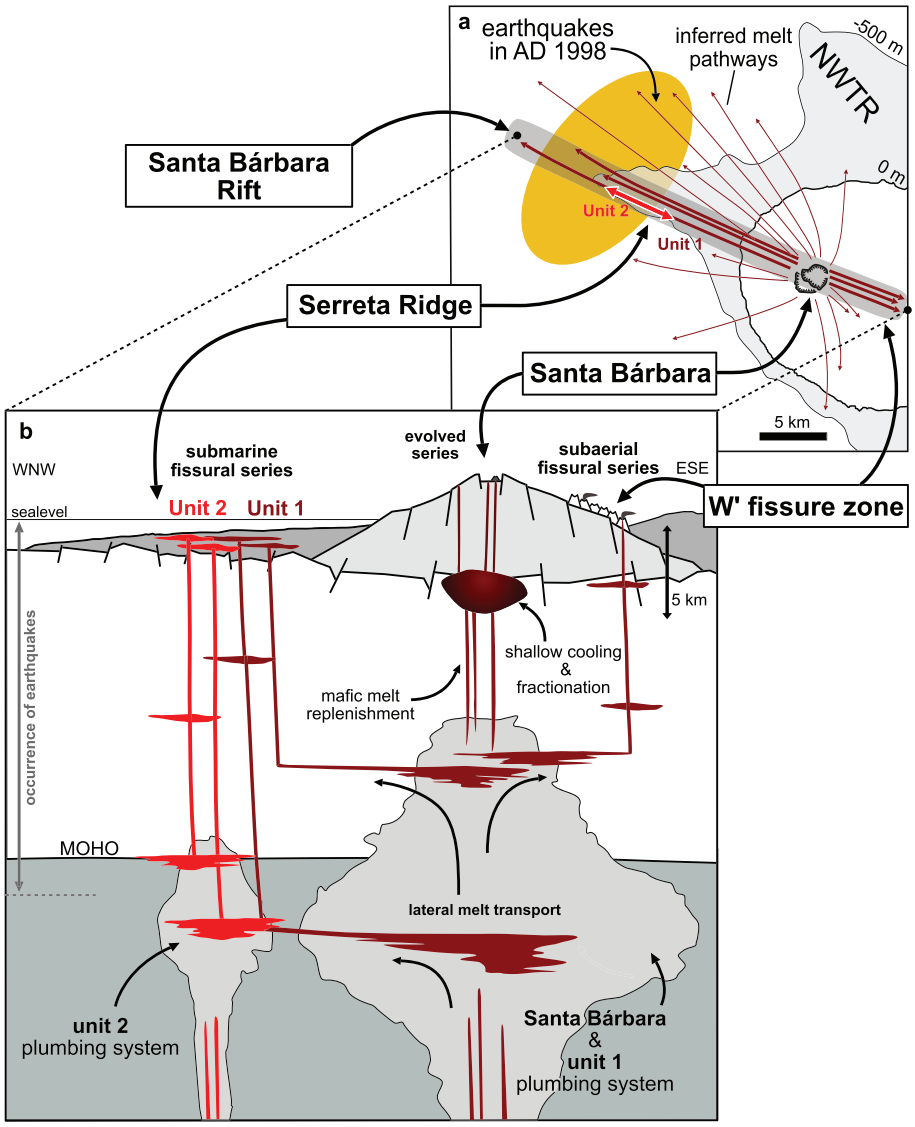

Figure 9. (a) Map of the western part of Terceira Island and the submarine Serreta Ridge. The dark red arrows schematically indicate the transport of melts from the Santa Bárbara plumbing system, whereas most melts are transported along the Santa Bárbara Rift and in ESE and WNW direction feeding Serreta unit 1. Additional melt transport occurs subordinately in variable directions radially around Santa Bárbara as indicated by thinner arrows. The red arrow schematically illustrates the magma pathway of the younger Serreta unit 2, which has a smaller spatial distribution than and is independent from lavas from the Santa Bárbara plumbing system. The plumbing systems beneath Santa Bárbara and Serreta Ridge (indicated by the grey fields) consist of a system of sills, melt pockets, crystal mush and crystallized intra-crustal magmatic bodies. The yellow field at Serreta Ridge highlights the area in which earthquakes occurred in 1998, which are interpreted as precursors for the Serreta eruption (Gaspar et al., 2015). (b) Schematic model for the emplacement and movement of melts feeding the Santa Bárbara volcano and units 1 and 2 of Serreta Ridge. Model represents a cross section along an ESE-WNW oriented profile forming the Santa Bárbara Rift. The Santa Bárbara plumbing system is a mature well-established system of sills, melts pockets and crystallized magmatic bodies. Melts feeding Santa Bárbara ascending through this plumbing get hampered and laterally expand into the fissure zone in predominantly WNW and ESE directions at depths >5 km forming unit 1. The occurrence of earthquakes in the lithosphere beneath Terceira is from Fontiela et al. (2018).

deep magmatic systems and melting regions beneath the islands are not fixed within a segment and relative to a central volcano. Within the past 400 ka four central volcanoes have formed on Terceira displaying a gradual shift of the central volcanoes toward west (Calvert et al., 2006; Hildenbrand et al., 2014). Thus, the formation of Serreta Ridge WNW of Santa Bárbara volcano likely is the result of this westward shift.

Lavas from Serreta Ridge cover a range from enriched melts with low degree of partial melting (unit 1) to depleted melts with higher degree of partial melting (unit 2). Combined with higher temperatures for unit 2 (Figure 6), we conclude that they reflect an early phase of volcanic activity in which melts ascend isolated from the Santa Bárbara plumbing systems, that is, unit 2 lavas can be regarded as the surface expression of an early phase of a young, immature melting zone and plumbing system. The locations of earthquakes' epicenters in CE 1998, interpreted as precursory seismic activity to the 1998–2001 Serreta eruption (Gaspar et al., 2003) are located exclusively beneath Serreta Ridge >10 km offshore Terceira (Gaspar et al., 2015) and not beneath Santa Bárbara volcano (Figure 9). This is evidence that differences in the geochemical signatures and temperature between Serreta unit 1 and 2 is the result of magma ascent in two independent plumbing systems. We conclude that unit 2 and potential stratigraphically deeper, unsampled equivalents reflect the presence of a young magma plumbing system in the mantle, which is located WNW of Santa Bárbara volcano. Whereas unit 1 reflects lateral flow of magmas from the Santa Bárbara volcano, the young eruption of unit 2 marks vertical magma ascent from the mantle. The young plumbing system beneath Serreta unit 2 probably heralds the early stage of a new central volcano.

6. Conclusions

The submarine Serreta Ridge west of the Azores island of Terceira forms a series of WNW-ESE oriented elongated eruptive centers, cones and fault scarps, which are part of the western Terceira magmatic system. Geochemical and structural signatures indicate that Serreta Ridge formed by focused melt transport and eruption in several phases erupting mafic to intermediate lavas. Differences in major and trace elements and isotope signatures show that submarine lavas originated from at least two distinct mantle sources. The youngest lava suite which is in part associated with the 1998–2001 Serreta eruption (unit 2) shows a geochemically more depleted source character than other submarine and subaerial lavas from western Terceira. In contrast, older submarine lava suites are isotopically similar to subaerial lavas from the Santa Bárbara volcano and W' fissure zone. They are interpreted to represent the mafic and submarine equivalent to Santa Bárbara. We interpret much of the spatial and temporal variability of the Serreta Ridge lavas to represent the transition from a rift system connected to the central volcano by lateral melt transport toward an independent small plumbing system with vertical melt transport.

The younger Serreta system might be the continuation of the general westward propagation of central volcanic centers observed on Terceira and other island in the Eastern Azores Plateau. This study demonstrates the importance of detailed geochemical investigation and magma pathways of ocean islands that are influenced and controlled by tectonic processes.

Acknowledgments
We acknowledge help and support from captains M. Schneider and J.F. Schubert, crews, and scientists during M113 and M128 for their invaluable, friendly support during the—at times difficult—operations. RR acknowledges the help of M. Regelous in the clean laboratories and during the trace element and isotope analyses. We acknowledge the constructive and helpful reviews by A. Pimentel and D. Geist and editorial handling by M. Edmonds. A special thanks to C. Hübscher, chief scientist of cruise M113 for providing the bathymetric data used in this study. ChB and RR acknowledge inspirational support by G. D. Mar and B. D. K. Schleifer. All data used in this study can be found in Tables S1 to S3 and all new data will be available on the PANGAEA data repository. This study was funded by the Deutsche Forschungsgemeinschaft (DFG grant BE4459/9-1).

References

Abdel-Monem, A. A., Fernandez, L. A., & Boone, G. M. (1975). K-Ar ages from the eastern Azores group (Santa Maria, São Miguel and the Formigas islands). *Lithos*, *8*(4), 247–254. https://doi.org/10.1016/0024-4937(75)90008-0

Acocella, V., & Neri, M. (2009). Dike propagation in volcanic edifices: overview and possible developments. *Tectonophysics*, *471*(1-2), 67–77. https://doi.org/10.1016/j.tecto.2008.10.002

Agranier, A., Blichert-Toft, J., Graham, D., Debaille, V., Schiano, P., & Albarède, F. (2005). The spectra of isotopic heterogeneities along the mid-Atlantic Ridge. *Earth and Planetary Science Letters*, *238*(1-2), 96–109. https://doi.org/10.1016/j.epsl.2005.07.011

Anderson, E. M. (1951). *The dynamics of faulting and dyke formation with applications to Britain*. London: Hafner Pub. Co.

Asimow, P. D., Dixon, J. E., & Langmuir, C. H. (2004). A hydrous melting and fractionation model for mid-ocean ridge basalts: Application to the Mid-Atlantic Ridge near the Azores. *Geochemistry, Geophysics, Geosystems*, *5*, Q01E16. https://doi.org/10.1029/2003GC000568

Béguelin, P., Bizimis, M., Beier, C., & Turner, S. (2017). Rift–plume interaction reveals multiple generations of recycled oceanic crust in Azores lavas. *Geochimica et Cosmochimica Acta*, *218*, 132–152. https://doi.org/10.1016/j.gca.2017.09.015

Beier, C., Brandl, P. A., Lima, S. M., & Haase, K. M. (2018). Tectonic control on the genesis of magmas in the New Hebrides arc (Vanuatu). *Lithos*, *312*, 290–307.

Beier, C., Haase, K. M., Abouchami, W., Krienitz, M. S., & Hauff, F. (2008). Magma genesis by rifting of oceanic lithosphere above anomalous mantle: Terceira Rift, Azores. *Geochemistry, Geophysics, Geosystems*, *9*, Q12013. https://doi.org/10.1029/2008GC002112

Beier, C., Haase, K. M., & Brandl, P. A. (2018). Melting and mantle sources in the Azores. In U. Kueppers, & C. Beier (Eds.), *Volcanoes of the Azores: Revealing the Geological Secrets of the Central Northern Atlantic Islands*, (pp. 251–280). Berlin, Heidelberg: Springer.

Beier, C., Haase, K. M., & Hansteen, T. H. (2006). Magma evolution of the Sete Cidades volcano, São Miguel, Azores. *Journal of Petrology*, *47*(7), 1375–1411. https://doi.org/10.1093/petrology/egl014

Beier, C., Haase, K. M., & Turner, S. P. (2012). Conditions of melting beneath the Azores. *Lithos*, *144*, 1–11.

Beier, C., Bach, w., Blum, M., Cerqueira, T. S., da Costa, I. R., Ferreira, P. J., et al. (2017). Azores Plateau - Cruise No. M128 - July 02, 2016 - July 27, 2016 - Ponta Delgada (Portugal) - Ponta Delgada (Portugal). METEOR-Berichte. DFG-Senatskommission für Ozeanographie, p. 41.

Bonatti, E. (1990). Not so hot" hot spots" in the oceanic mantle. *Science*, *250*(4977), 107–111. https://doi.org/10.1126/science.250.4977.107

Bourdon, B., Turner, S. P., & Ribe, N. M. (2005). Partial melting and upwelling rates beneath the Azores from a U-series isotope perspective. *Earth and Planetary Science Letters*, *239*(1-2), 42–56. https://doi.org/10.1016/j.epsl.2005.08.008

Brandl, P. A., Beier, C., Regelous, M., Abouchami, W., Haase, K. M., Garbe-Schönberg, D., & Galer, S. J. G. (2012). Volcanism on the flanks of the East Pacific Rise: Quantitative constraints on mantle heterogeneity and melting processes. *Chemical Geology*, *298*, 41–56.

Burchardt, S., Walter, T. R., & Tuffen, H. (2018). Growth of a Volcanic Edifice Through Plumbing System Processes—Volcanic Rift Zones, Magmatic Sheet-Intrusion Swarms and Long-Lived Conduits. In *Volcanic and Igneous Plumbing Systems*, (pp. 89–112). Amsterdam: Elsevier.

Calvert, A. T., Moore, R. B., McGeehin, J. P., da Silva, A., & Rodrigues, M. (2006). Volcanic history and $^{40}Ar/^{39}$ Ar and ^{14}C geochronology of Terceira Island, Azores, Portugal. *Journal of Volcanology and Geothermal Research*, *156*(1-2), 103–115. https://doi.org/10.1016/j.jvolgeores.2006.03.016

Cannat, M., Briais, A., Deplus, C., Escartín, J., Georgen, J., Lin, J., et al. (1999). Mid-Atlantic Ridge–Azores hotspot interactions: along-axis migration of a hotspot-derived event of enhanced magmatism 10 to 4 Ma ago. *Earth and Planetary Science Letters*, *173*(3), 257–269. https://doi.org/10.1016/S0012-821X(99)00234-4

Casalbore, D., Romagnoli, C., Pimentel, A., Quartau, R., Casas, D., Ercilla, G., et al. (2015). Volcanic, tectonic and mass-wasting processes offshore Terceira Island (Azores) revealed by high-resolution seafloor mapping. *Bulletin of Volcanology*, *77*(3), 24. https://doi.org/10.1007/s00445-015-0905-3

Casas, D., Pimentel, A., Pacheco, J., Martorelli, E., Sposato, A., Ercilla, G., et al. (2018). Serreta 1998–2001 submarine volcanic eruption, offshore Terceira (Azores): Characterization of the vent and inferences about the eruptive dynamics. *Journal of Volcanology and Geothermal Research*, *356*, 127–140. https://doi.org/10.1016/j.jvolgeores.2018.02.017

Chadwick, W. W. Jr., & Dieterich, J. H. (1995). Mechanical modeling of circumferential and radial dike intrusion on Galapagos volcanoes. *Journal of Volcanology and Geothermal Research*, *66*(1-4), 37–52. https://doi.org/10.1016/0377-0273(94)00060-T

Chauvel, C., Bureau, S., & Poggi, C. (2011). Comprehensive chemical and isotopic analyses of basalt and sediment reference materials. *Geostandards and Geoanalytical Research*, *35*(1), 125–143. https://doi.org/10.1111/j.1751-908X.2010.00086.x

Chiocci, F. L., Romagnoli, C., Casalbore, D., Sposato, A., Martorelli, E., Alonso, B., et al. (2013). Bathy-morphological setting of Terceira Island (Azores) after the FAIVI cruise. *Journal of Maps*, *9*(4), 590–595. https://doi.org/10.1080/17445647.2013.831381

Compston, W., & Oversby, V. M. (1969). Lead isotopic analysis using a double spike. *Journal of Geophysical Research*, *74*(17), 4338–4348. https://doi.org/10.1029/JB074i017p04338

Dias, N. A., Matias, L., Lourenço, N., Madeira, J., Carrilho, F., & Gaspar, J. L. (2007). Crustal seismic velocity structure near Faial and Pico Islands (AZORES), from local earthquake tomography. *Tectonophysics*, *445*(3), 301–317. https://doi.org/10.1016/j.tecto.2007.09.001

D'Oriano, C., Landi, P., Pimentel, A., & Zanon, V. (2017). Magmatic processes revealed by anorthoclase textures and trace element modeling: The case of the Lajes Ignimbrite eruption (Terceira Island, Azores). *Journal of Volcanology and Geothermal Research*, *347*, 44–63. https://doi.org/10.1016/j.jvolgeores.2017.08.012

Dosso, L., Bougault, H., Langmuir, C., Bollinger, C., Bonnier, O., & Etoubleau, J. (1999). The age and distribution of mantle heterogeneity along the Mid-Atlantic Ridge (31–41 N). *Earth and Planetary Science Letters*, *170*(3), 269–286. https://doi.org/10.1016/S0012-821X(99)00109-0

Elliott, T., Blichert-Toft, J., Heumann, A., Koetsier, G., & Forjaz, V. (2007). The origin of enriched mantle beneath Sao Miguel, Azores. *Geochimica et Cosmochimica Acta*, *71*(1), 219–240. https://doi.org/10.1016/j.gca.2006.07.043

Feraud, G., Kaneoka, I., & Allègre, C. J. (1980). K/Ar ages and stress pattern in the Azores: Geodynamic implications. *Earth and Planetary Science Letters*, *46*(2), 275–286. https://doi.org/10.1016/0012-821X(80)90013-8

Fiske, R. S., & Jackson, E. D. (1972). Orientation and growth of Hawaiian volcanic rifts: The effect of regional structure and gravitational stresses. *Proceedings of the Royal Society of London*, *329*(1578), 299–326. https://doi.org/10.1098/rspa.1972.0115

Fontiela, J., Oliveira, C. S., & Rosset, P. (2018). Characterisation of Seismicity of the Azores Archipelago: An Overview of Historical Events and a Detailed Analysis for the Period 2000–2012. In U. Kueppers, & C. Beier (Eds.), *Volcanoes of the Azores: Revealing the Geological Secrets of the Central Northern Atlantic Islands*, (pp. 127–153). Berlin, Heidelberg: Springer.

Freund, S., Beier, C., Krumm, S., & Haase, K. M. (2013). Oxygen isotope evidence for the formation of andesitic–dacitic magmas from the fast-spreading Pacific–Antarctic Rise by assimilation–fractional crystallisation. *Chemical Geology*, *347*, 271–283. https://doi.org/10.1016/j.chemgeo.2013.04.013

Furumoto, A. S. (1978). Nature of the magma conduit under the East Rift Zone of Kilauea Volcano, Hawaii. *Bulletin Volcanologique*, *41*(4), 435–453. https://doi.org/10.1007/BF02597376

Gale, A., Escrig, S., Gier, E. J., Langmuir, C. H., & Goldstein, S. L. (2011). Enriched basalts at segment centers: The Lucky Strike (37 17′ N) and Menez Gwen (37 50′ N) segments of the Mid-Atlantic Ridge. *Geochemistry, Geophysics, Geosystems*, *12*, Q06016. https://doi.org/10.1029/2010GC003446

Gale, A., Laubier, M., Escrig, S., & Langmuir, C. H. (2013). Constraints on melting processes and plume-ridge interaction from comprehensive study of the FAMOUS and North Famous segments, Mid-Atlantic Ridge. *Earth and Planetary Science Letters*, *365*, 209–220. https://doi.org/10.1016/j.epsl.2013.01.022

Garcia, M. O., Rhodes, J. M., Trusdell, F. A., & Pietruszka, A. J. (1996). Petrology of lavas from the Puu Oo eruption of Kilauea Volcano: III. The Kupaianaha episode (1986–1992). *Bulletin of Volcanology*, *58*(5), 359–379. https://doi.org/10.1007/s004450050145

Gaspar, J. L., Queiroz, G., Ferreira, T., Medeiros, A. R., Goulart, C., & Medeiros, J. (2015). Earthquakes and volcanic eruptions in the Azores region: Geodynamic implications from major historical events and instrumental seismicity, Geological Society, London. *Memoirs*, *44*(1), 33–49. https://doi.org/10.1144/M44.4

Gaspar, J. L., Queiroz, G., Pacheco, J. M., Ferreira, T., Wallenstein, N., Almeida, M. H., & Coutinho, R. (2003). Basaltic lava balloons produced during the 1998–2001 Serreta Submarine Ridge eruption (Azores). *Explosive subaqueous volcanism*, *140*, 205–212. https://doi.org/10.1029/140GM13

Geist, D., Howards, K. A., & Larson, P. (1995). The Generation of Oceanic Rhyolites by Crystal Fractionation: The Basalt-Rhyolite Association at Volcán Alcedo, Galápagos Archipelago. *Journal of Petrology*, *36*(4), 965–982. https://doi.org/10.1093/petrology/36.4.965

Geist, D. J., Fornari, D. J., Kurz, M. D., Harpp, K. S., Soule, S. A., Perfit, M. R., & Koleszar, A. M. (2006). Submarine Fernandina: Magmatism at the leading edge of the Galápagos hot spot. *Geochemistry, Geophysics, Geosystems*, *7*, Q12007. https://doi.org/10.1029/2006GC001290

Gente, P., Dyment, J., Maia, M., & Goslin, J. (2003). Interaction between the Mid-Atlantic Ridge and the Azores hot spot during the last 85 Myr: Emplacement and rifting of the hot spot-derived plateaus. *Geochemistry, Geophysics, Geosystems*, *4*(10), 8514. https://doi.org/10.1029/2003GC000527

Gertisser, R., Self, S., Gaspar, J. L., Kelley, S. P., Pimentel, A., Eikenberg, J., et al. (2010). Ignimbrite stratigraphy and chronology on Terceira Island, Azores. *The Geological Society of America, Special Paper*, *464*, 133–154.

Gibson, S. A., & Geist, D. (2010). Geochemical and geophysical estimates of lithospheric thickness variation beneath Galápagos. *Earth and Planetary Science Letters*, *300*(3-4), 275–286. https://doi.org/10.1016/j.epsl.2010.10.002

Gudmundsson, A. (2000). Dynamics of Volcanic Systems in Iceland: Example of Tectonism and Volcanism at Juxtaposed Hot Spot and Mid-Ocean Ridge Systems. *Annual Review of Earth and Planetary Sciences*, *28*(1), 107–140. https://doi.org/10.1146/annurev.earth.28.1.107

Gudmundsson, A. (2006). How local stresses control magma-chamber ruptures, dyke injections, and eruptions in composite volcanoes. *Earth-Science Reviews*, *79*(1-2), 1–31. https://doi.org/10.1016/j.earscirev.2006.06.006

Gudmundsson, A., Lecoeur, N., Mohajeri, N., & Thordarson, T. (2014). Dike emplacement at Bardarbunga, Iceland, induces unusual stress changes, caldera deformation, and earthquakes. *Bulletin of Volcanology*, *76*(10), 869. https://doi.org/10.1007/s00445-014-0869-8

Haase, K. M., Beier, C., Regelous, M., Rapprich, V., & Renno, A. (2017). Spatial variability of source composition and petrogenesis in rift and rift flank alkaline lavas from the Eger Rift, Central Europe. *Chemical Geology*, *455*(Supplement C), 304–314. https://doi.org/10.1016/j.chemgeo.2016.11.003

Haase, K. M., Regelous, M., Duncan, R. A., Brandl, P. A., Stroncik, N., & Grevemeyer, I. (2011). Insights into mantle composition and mantle melting beneath mid-ocean ridges from postspreading volcanism on the fossil Galapagos Rise. *Geochemistry, Geophysics, Geosystems*, *12*, Q0AC11. https://doi.org/10.1029/2010GC003482

Hamelin, C., Bezos, A., Dosso, L., Escartin, J., Cannat, M., & Mevel, C. (2013). Atypically depleted upper mantle component revealed by Hf isotopes at Lucky Strike segment. *Chemical Geology*, *341*, 128–139. https://doi.org/10.1016/j.chemgeo.2013.01.013

Hildenbrand, A., Madureira, P., Marques, F. O., Cruz, I., Henry, B., & Silva, P. (2008). Multi-stage evolution of a sub-aerial volcanic ridge over the last 1.3 Myr: S. Jorge Island, Azores Triple Junction. *Earth and Planetary Science Letters*, *273*(3-4), 289–298. https://doi.org/10.1016/j.epsl.2008.06.041

Hildenbrand, A., Marques, F. O., Costa, A. C. G., Sibrant, A. L. R., Silva, P. F., Henry, B., et al. (2012). Reconstructing the architectural evolution of volcanic islands from combined K/Ar, morphologic, tectonic, and magnetic data: The Faial Island example (Azores). *Journal of Volcanology and Geothermal Research*, *241*, 39–48.

Hildenbrand, A., Weis, D., Madureira, P., & Marques, F. O. (2014). Recent plate re-organization at the Azores Triple Junction: Evidence from combined geochemical and geochronological data on Faial, S. Jorge and Terceira volcanic islands. *Lithos*, *210*, 27–39.

Hollingsworth, J., Leprince, S., Ayoub, F., & Avouac, J. P. (2012). Deformation during the 1975–1984 Krafla rifting crisis, NE Iceland, measured from historical optical imagery. *Journal of Geophysical Research*, *117*, B11407. https://doi.org/10.1029/2012JB009140

Hübscher, C. Beier, C., Al-Hseinat, M., Batista, L., Blum, M., Bobsin, M., et al., (2016), Azores Plateau – Cruise No. M113/1 – December 29, 2014 – January 22, 2015 – Ponta Delgada (Portugal) – Ponta Delgada (Portugal), METEOR-Berichte. DFG-Senatskommission für Ozeanographie, p. 31, doi:10.2312/cr_m113_1.

Jeffery, A. J., & Gertisser, R. (2018). Peralkaline felsic magmatism of the Atlantic islands. *Frontiers in Earth Science*, *6*, 145.

Jeffery, A. J., Gertisser, R., O'Driscoll, B., Pacheco, J. M., Whitley, S., Pimentel, A., & Self, S. (2016). Temporal evolution of a post-caldera, mildly peralkaline magmatic system: Furnas volcano, São Miguel, Azores. *Contributions to Mineralogy and Petrology*, *171*(5), 42. https://doi.org/10.1007/s00410-016-1235-y

Jeffery, A. J., Gertisser, R., Self, S., Pimentel, A., O'driscoll, B., & Pacheco, J. M. (2017). Petrogenesis of the peralkaline ignimbrites of Terceira, Azores. *Journal of Petrology*, *58*(12), 2365–2402. https://doi.org/10.1093/petrology/egy012

Jochum, K. P., Willbold, M., Raczek, I., Stoll, B., & Herwig, K. (2005). Chemical Characterisation of the USGS Reference Glasses GSA-1G, GSC-1G, GSD-1G, GSE-1G, BCR-2G, BHVO-2G and BIR-1G Using EPMA, ID-TIMS, ID-ICP-MS and LA-ICP-MS. *Geostandards and Geoanalytical Research*, *29*(3), 285–302.

Johnson, C. L., Wijbrans, J. R., Constable, C. G., Gee, J., Staudigel, H., Tauxe, L., et al. (1998). 40Ar/39Ar ages and paleomagnetism of São Miguel lavas, Azores. *Earth and Planetary Science Letters*, *160*(3), 637–649. https://doi.org/10.1016/S0012-821X(98)00117-4

Klügel, A., Hansteen, T. H., & Galipp, K. (2005). Magma storage and underplating beneath Cumbre Vieja volcano, la Palma (Canary Islands). *Earth and Planetary Science Letters*, *236*(1-2), 211–226. https://doi.org/10.1016/j.epsl.2005.04.006

Klügel, A., Longpré, M.-A., García-Cañada, L., & Stix, J. (2015). Deep intrusions, lateral magma transport and related uplift at ocean island volcanoes. *Earth and Planetary Science Letters*, *431*, 140–149. https://doi.org/10.1016/j.epsl.2015.09.031

Klügel, A., Walter, T. R., Schwarz, S., & Geldmacher, J. (2005). Gravitational spreading causes en-echelon diking along a rift zone of Madeira Archipelago: An experimental approach and implications for magma transport. *Bulletin of Volcanology*, *68*(1), 37–46. https://doi.org/10.1007/s00445-005-0418-6

Kueppers, U., Nichols, A. R. L., Zanon, V., Potuzak, M., & Pacheco, J. M. R. (2012). Lava balloons—peculiar products of basaltic submarine eruptions. *Bulletin of Volcanology*, *74*(6), 1379–1393. https://doi.org/10.1007/s00445-012-0597-x

Larrea, P., França, Z., Widom, E., & Lago, M. (2018). Petrology of the Azores Islands. In U. Kueppers, & C. Beier (Eds.), *Volcanoes of the Azores: Revealing the Geological Secrets of the Central Northern Atlantic Islands*, (pp. 197–249). Berlin, Heidelberg: Springer.

Larrea, P., Galé, C., Ubide, T., Widom, E., Lago, M., & França, Z. (2014). Magmatic Evolution of Graciosa (Azores, Portugal). *Journal of Petrology*, *55*(11), 2125–2154. https://doi.org/10.1093/petrology/egu052

Lourenço, N., Miranda, J. M., Luis, J., Ribeiro, A., Mendes Victor, L. A., Madeira, J., & Needham, H. D. (1998). Morpho-tectonic analysis of the Azores Volcanic Plateau from a new bathymetric compilation of the area. *Marine Geophysical Researches*, *20*(3), 141–156. https://doi.org/10.1023/A:1004505401547

Madeira, J., Brum da Silveira, A., Hipólito, A., & Carmo, R. (2015). Active tectonics in the Central and Eastern Azores Islands along the Eurasia–Nubia boundary: A review, Geological Society, London. *Memoirs*, *44*(1), 15–32. https://doi.org/10.1144/M44.3

Madureira, P., Mata, J., Mattielli, N., Queiroz, G., & Silva, P. (2011). Mantle source heterogeneity, magma generation and magmatic evolution at Terceira Island (Azores archipelago): Constraints from elemental and isotopic (Sr, Nd, Hf, and Pb) data. *Lithos*, *126*(3-4), 402–418. https://doi.org/10.1016/j.lithos.2011.07.002

Madureira, P., Moreira, M., & Mata, J. (2005). The Azores hotspot: A lower mantle origin for Terceira magmas as shown by Ne isotopic data. *Geochimica et Cosmochimica Acta*, *69*(10).

Madureira, P., Rosa, C., Marques, A. F., Silva, P., Moreira, M., Hamelin, C., et al. (2017). The 1998–2001 submarine lava balloon eruption at the Serreta ridge (Azores archipelago): Constraints from volcanic facies architecture, isotope geochemistry and magnetic data. *Journal of Volcanology and Geothermal Research*, *329*, 13–29. https://doi.org/10.1016/j.jvolgeores.2016.11.006

Marques, F., Catalão, J., Hildenbrand, A., & Madureira, P. (2015). Ground motion and tectonics in the Terceira Island: Tectonomagmatic interactions in an oceanic rift (Terceira Rift, Azores Triple Junction). *Tectonophysics*, *651*, 19–34.

Marques, F. O., Catalão, J. C., DeMets, C., Costa, A. C. G., & Hildenbrand, A. (2013). GPS and tectonic evidence for a diffuse plate boundary at the Azores Triple Junction. *Earth and Planetary Science Letters*, *381*(Supplement C), 177–187. https://doi.org/10.1016/j.epsl.2013.08.051

Masotta, M., Mollo, S., Freda, C., Gaeta, M., & Moore, G. (2013). Clinopyroxene–liquid thermometers and barometers specific to alkaline differentiated magmas. *Contributions to Mineralogy and Petrology*, *166*(6), 1545–1561. https://doi.org/10.1007/s00410-013-0927-9

McGuire, W., & Pullen, A. (1989). Location and orientation of eruptive fissures and feederdykes at Mount Etna; influence of gravitational and regional tectonic stress regimes. *Journal of Volcanology and Geothermal Research*, *38*(3-4), 325–344. https://doi.org/10.1016/0377-0273(89)90046-2

Menand, T. (2011). Physical controls and depth of emplacement of igneous bodies: A review. *Tectonophysics*, *500*(1-4), 11–19. https://doi.org/10.1016/j.tecto.2009.10.016

Métrich, N., Zanon, V., Créon, L., Hildenbrand, A., Moreira, M., & Marques, F. O. (2014). Is the 'Azores hotspot'a wetspot? Insights from the geochemistry of fluid and melt inclusions in olivine of Pico basalts. *Journal of Petrology*, *55*(2), 377–393. https://doi.org/10.1093/petrology/egt071

Millet, M.-A., Doucelance, R., Baker, J. A., & Schiano, P. (2009). Reconsidering the origins of isotopic variations in Ocean Island Basalts: Insights from fine-scale study of São Jorge Island, Azores archipelago. *Chemical Geology*, *265*(3-4), 289–302. https://doi.org/10.1016/j.chemgeo.2009.04.005

Miranda, J. M., Luis, J. F., & Lourenço, N. (2018). The Tectonic Evolution of the Azores Based on Magnetic Data. In U. Kueppers, & C. Beier (Eds.), *Volcanoes of the Azores: Revealing the Geological Secrets of the Central Northern Atlantic Islands*, (pp. 89–100). Berlin, Heidelberg: Springer.

Mitchell, N. C. (2001). Transition from circular to stellate forms of submarine volcanoes. *Journal of Geophysical Research*, *106*(B2), 1987–2003. https://doi.org/10.1029/2000JB900263

Mjelde, R., Wessel, P., & Müller, R. D. (2010). Global pulsations of intraplate magmatism through the Cenozoic. *Lithosphere*, *2*(5), 361–376. https://doi.org/10.1130/l107.1

Moore, R. B. (1990). Volcanic geology and eruption frequency, São Miguel, Azores. *Bulletin of Volcanology*, *52*(8), 602–614. https://doi.org/10.1007/bf00301211

Moreira, M. A., Geoffroy, L., & Pozzi, J. P. (2015). Magma flow pattern in dykes of the Azores revealed by anisotropy of magnetic susceptibility. *Journal of Geophysical Research: Solid Earth*, *120*, 662–690. https://doi.org/10.1002/2014JB010982

Mungall, J. E., & Martin, R. F. (1995). Petrogenesis of basalt-comendite and basalt-pantellerite suites, Terceira, Azores, and some implications for the origin of ocean-island rhyolites. *Contributions to Mineralogy and Petrology*, *119*(1), 43–55. https://doi.org/10.1007/BF00310716

Navarro, A., Lourenço, N., Chorowicz, J., Miranda, J. M., & Catalão, J. (2009). Analysis of geometry of volcanoes and faults in Terceira Island (Azores): Evidence for reactivation tectonics at the EUR/AFR plate boundary in the Azores triple junction. *Tectonophysics*, *465*(1-4), 98–113. https://doi.org/10.1016/j.tecto.2008.10.020

Neave, D. A., & Putirka, K. D. (2017). A new clinopyroxene-liquid barometer, and implications for magma storage pressures under Icelandic rift zones. *American Mineralogist*, *102*(4), 777–794. https://doi.org/10.2138/am-2017-5968

Neves, M., Miranda, J., & Luis, J. (2013). The role of lithospheric processes on the development of linear volcanic ridges in the Azores. *Tectonophysics*, *608*, 376–388. https://doi.org/10.1016/j.tecto.2013.09.016

Nunes, J. C., A. Calvert, S. Medeiros, E. A. Lima, F. Pereira, M. P. Costa, et al. (2014), Geological mapping of the central area of Terceira Island (Azores, Portugal): Associated volcanostratigraphy, ages and genetic implications on the Malha-Balcões-Chamusca lava caves system, Comunicações Geológicas, 101, Especial I, 283-288.

O'Neill, C., & Sigloch, K. (2018). Crust and Mantle Structure Beneath the Azores Hotspot—Evidence from Geophysics. In U. Kueppers, & C. Beier (Eds.), *Volcanoes of the Azores: Revealing the Geological Secrets of the Central Northern Atlantic Islands*, (pp. 71–87). Berlin, Heidelberg: Springer.

Pietruszka, A. J., Marske, J. P., Heaton, D. E., Garcia, M. O., & Rhodes, J. M. (2018). An Isotopic Perspective into the Magmatic Evolution and Architecture of the Rift Zones of Kīlauea Volcano. *Journal of Petrology*, *59*(12), 2311–2352. https://doi.org/10.1093/petrology/egy098

Pimentel, A., Zanon, V., de Groot, L. V., Hipólito, A., di Chiara, A., & Self, S. (2016). Stress-induced comenditic trachyte effusion triggered by trachybasalt intrusion: Multidisciplinary study of the AD 1761 eruption at Terceira Island (Azores). *Bulletin of Volcanology*, *78*(3), 22. https://doi.org/10.1007/s00445-016-1015-6

Putirka, K. D. (1999). Clinopyroxene+ liquid equilibria to 100 kbar and 2450 K. *Contributions to Mineralogy and Petrology*, *135*(2-3), 151–163. https://doi.org/10.1007/s004100050503

Putirka, K. D. (2008). Thermometers and barometers for volcanic systems. *Reviews in Mineralogy and Geochemistry*, *69*(1), 61–120. https://doi.org/10.2138/rmg.2008.69.3

Putirka, K. D., Mikaelian, H., Ryerson, F., & Shaw, H. (2003). New clinopyroxene-liquid thermobarometers for mafic, evolved, and volatile-bearing lava compositions, with applications to lavas from Tibet and the Snake River Plain, Idaho. *American Mineralogist*, *88*(10), 1542–1554. https://doi.org/10.2138/am-2003-1017

Quartau, R., Hipólito, A., Romagnoli, C., Casalbore, D., Madeira, J., Tempera, F., et al. (2014). The morphology of insular shelves as a key for understanding the geological evolution of volcanic islands: Insights from Terceira Island (Azores). *Geochemistry, Geophysics, Geosystems*, *15*, 1801–1826. https://doi.org/10.1002/2014GC005248

Romer, R. H. W., Beier, C., Haase, K. M., & Hübscher, C. (2018). Correlated changes between volcanic structures and magma composition in the Faial volcanic system, Azores. *Frontiers in Earth Science*, *6*, 78. https://doi.org/10.3389/feart.2018.00078

Schilling, J.-G. (1975). Azores mantle blob: Rare-earth evidence. *Earth and Planetary Science Letters*, *25*(2), 103–115. https://doi.org/10.1016/0012-821X(75)90186-7

Schilling, J.-G., Bergeron, M. B., Evans, R., & Smith, J. V. (1980). Halogens in the mantle beneath the north atlantic [and discussion]. *Philosophical Transactions of the Royal Society of London A: Mathematical, Physical and Engineering Sciences*, *297*(1431), 147–178. https://doi.org/10.1098/rsta.1980.0208

Self, S. (1976). The recent volcanology of Terceira, Azores. *Journal of the Geological Society*, *132*(6), 645–666. https://doi.org/10.1144/gsjgs.132.6.0645

Self, S., & Gunn, B. M. (1976). Petrology, volume and age relations of alkaline and saturated peralkaline volcanics from Terceira, Azores. *Contributions to Mineralogy and Petrology*, *54*(4), 293–313. https://doi.org/10.1007/BF00389409

Shirey, S. B., Bender, J. F., & Langmuir, C. H. (1987). Three-component isotopic heterogeneity near the Oceanographer transform, Mid-Atlantic Ridge. *Nature*, *325*(6101), 217–223. https://doi.org/10.1038/325217a0

Sibrant, A. L. R., Marques, F. O., & Hildenbrand, A. (2014). Construction and destruction of a volcanic island developed inside an oceanic rift: Graciosa Island, Terceira Rift, Azores. *Journal of Volcanology and Geothermal Research*, *284*, 32–45. https://doi.org/10.1016/j.jvolgeores.2014.07.014

Sigmarsson, O., & Halldórsson, S. A. (2015). Delimiting Bárðarbunga and Askja volcanic systems with Sr-and Nd-isotope ratios. *Jökull*, *65*, 17–27.

Smith, D. K., & Cann, J. R. (1993). Building the crust at the Mid-Atlantic Ridge. *Nature*, *365*(6448), 707–715. https://doi.org/10.1038/365707a0

Spieker, K., Rondenay, S., Ramalho, R., Thomas, C., & Helffrich, G. (2018). Constraints on the structure of the crust and lithosphere beneath the Azores Islands from teleseismic receiver functions. *Geophysical Journal International*, *213*(2), 824–835. https://doi.org/10.1093/gji/ggy022

Tilling, R. I., & Dvorak, J. J. (1993). Anatomy of a basaltic volcano. *Nature*, *363*(6425), 125–133. https://doi.org/10.1038/363125a0

Vervoort, J. D., & Blichert-Toft, J. (1999). Evolution of the depleted mantle: Hf isotope evidence from juvenile rocks through time. *Geochimica et Cosmochimica Acta*, *63*(3-4), 533–556. https://doi.org/10.1016/S0016-7037(98)00274-9

Vogt, P. R., & Jung, W. Y. (2004). The Terceira Rift as hyper-slow, hotspot-dominated oblique spreading axis: A comparison with other slow-spreading plate boundaries. *Earth and Planetary Science Letters*, *218*(1-2), 77–90. https://doi.org/10.1016/S0012-821X(03)00627-7

Walker, G. P. L. (1999). Volcanic rift zones and their intrusion swarms. *Journal of Volcanology and Geothermal Research*, *94*(1-4), 21–34. https://doi.org/10.1016/S0377-0273(99)00096-7

Weiß, B. J., Hübscher, C., Wolf, D., & Lüdmann, T. (2015). Submarine explosive volcanism in the southeastern Terceira Rift/São Miguel region (Azores). *Journal of Volcanology and Geothermal Research*, *303*, 79–91. https://doi.org/10.1016/j.jvolgeores.2015.07.028

White, W. M., Schilling, J. G., & Hart, S. R. (1976). Evidence for Azores Mantle Plume from Strontium Isotope Geochemistry of Central North-Atlantic. *Nature*, *263*(5579), 659–663. https://doi.org/10.1038/263659a0

Woelki, D., Regelous, M., Haase, K. M., Romer, R. H. W., & Beier, C. (2018). Petrogenesis of boninitic lavas from the Troodos Ophiolite, and comparison with Izu–Bonin–Mariana fore-arc crust. *Earth and Planetary Science Letters*, *498*, 203–214. https://doi.org/10.1016/j.epsl.2018.06.041

Zanon, V., & Frezzotti, M. L. (2013). Magma storage and ascent conditions beneath Pico and Faial islands (Azores archipelago): A study on fluid inclusions. *Geochemistry, Geophysics, Geosystems*, *14*, 3494–3514. https://doi.org/10.1002/ggge.20221

Zanon, V., & Pimentel, A. (2015). Spatio-temporal constraints on magma storage and ascent conditions in a transtensional tectonic setting: The case of the Terceira Island (Azores). *American Mineralogist*, *100*(4), 795–805. https://doi.org/10.2138/am-2015-4936